

AD719294



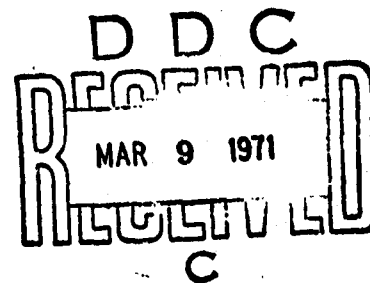
COAST GUARD

OFFICE OF RESEARCH & DEVELOPMENT

CONTRACT DOT-CG-00,504-A

STUDIES OF OIL RETENTION BOOM HYDRODYNAMICS

W. T. LINDENMUTH
E. R. MILLER, JR.
C. C. HSU



HYDRONAUTICS, INCORPORATED
PINDELL SCHOOL ROAD, HOWARD COUNTY
LAUREL, MARYLAND 20810

Best Available Copy

DECEMBER 1970

FINAL REPORT

Prepared for: **COMMANDANT (DAT)**
U.S. COAST GUARD HEADQUARTERS
WASHINGTON, D.C., 20591

Reproduced by
**NATIONAL TECHNICAL
INFORMATION SERVICE**
Springfield, Va. 22151

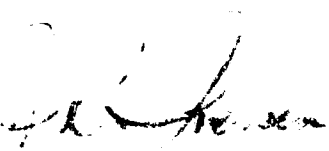
DISTRIBUTION STATEMENT A
Approved for public release;
Distribution Unlimited

DATE: JAN 18 1971

This report has been submitted in fulfillment of contract DOT-CG-00,504-A and is promulgated subject to the following qualifications:

The contents of this report reflect the views of Hydronautics, Inc.

which is responsible for the facts and the accuracy of the data presented herein. The contents do not necessarily reflect the official views or policy of the Coast Guard. This report does not constitute a standard, specification or regulation.



J. R. IVERSEN
Captain, U. S. Coast Guard
Chief, Applied Technology Division
Office of Research and Development
U. S. Coast Guard Headquarters
Washington, D. C. 20591

| | | |
|--|---|---|
| 1. Report No. 714102/A-1008 | 2. Government Accession No. | 3. Rept. No. / Catalog No. |
| 4. Title and Subtitle STUDIES OF OIL CONTAINMENT BOOM HYDRODYNAMICS | 5. Report Date December 1970 | 6. Performing Organization Code |
| 7. Author(s) William T. Lindenmuth, E.R. Miller, C.C. Hsiao | 8. Performing Organization Report No. 7013-2 | 9. Work Unit No. |
| 9. Performing Organization Name and Address HYDRONAUTICS, Incorporated Findell School Road, Howard County Laurel, Maryland 20810 | 10. Contract or Grant No. DOT-CG-00504-A | 11. Type of Report and Period Covered Final Technical Report |
| 12. Sponsoring Agency Name and Address United States Coast Guard Department of Transportation Washington, D. C. | 13. Sponsoring Agency Code | |
| 14. Supplementary Notes | | |
| 15. Abstract <p>Results of an experimental investigation of oil containment hydrodynamics are presented with theoretical analyses to help explain the experimental findings. Two-dimensional model tests were performed using several petroleum products including diesel fuel and motor oil. Test variables in addition to oil properties were current, interfacial tension, gravity waves, slick volume, containment boom geometry, and boom depth. Also studied were three-dimensional effects and the efficiency of using absorbent additives and multiple boom configurations as containment aids.</p> | | |
| 17. Key Words Pollution Oil Booms Oil Spills | 18. Distribution Statement Distribution of this document is unlimited. | |
| 19. Security Classification (of this report) UNCLASSIFIED | 20. Security Classification (of this page) UNCLASSIFIED | 21. No. of Pages 121 |
| 22. Price | | |

REPORT NO. 714102/A/008

STUDIES OF OIL RETENTION BOOM HYDRODYNAMICS

CONTRACT DOT-CO-00504-A

**William T. Lindenmuth,
Eugene R. Miller, Jr., and C. C. Hsu**

**HYDRONAUTICS, Incorporated
Vindell School Road, Howard County
Laurel, Maryland 20810**

December 1970

FINAL REPORT

**Availability is unlimited. Document may be released to the
Clearinghouse for Federal Scientific and Technical Information,
Springfield, Virginia 22151, for sale to the public.**

TABLE OF CONTENTS

| | Page |
|---|------|
| I. INTRODUCTION..... | 1 |
| II. SUMMARY OF OIL SLICK HYDRODYNAMICS..... | 7 |
| A. The Headwave..... | 7 |
| B. Oil Slick Setup..... | 9 |
| 1. Wind and Current..... | 9 |
| 2. Waves..... | 11 |
| C. Entrainment..... | 13 |
| 1. Droplet Formation..... | 13 |
| 2. Droplet Rise..... | 15 |
| 3. Entrainment Loss..... | 20 |
| 4. Effect of Waves on Entrainment Loss..... | 25 |
| D. Drainage..... | 27 |
| E. Scale Model Testing..... | 29 |
| 1. Scaling Parameters..... | 29 |
| 2. Expansion of Typical Model Test Data..... | 31 |
| 3. Conclusions with Respect to Scale Model Tests..... | 37 |
| III. MODEL TEST EQUIPMENT AND PROCEDURES..... | 39 |
| A. Equipment..... | 39 |
| B. Models..... | 40 |
| C. Properties of Test Materials..... | 41 |
| D. Procedures..... | 42 |
| E. Observations..... | 43 |

TABLE OF CONTENTS (Concluded)

| | Page |
|---|------|
| IV. DISCUSSION OF TEST RESULTS..... | 44 |
| A. Studies of Headwave Geometry and Propagation..... | 44 |
| B. Oil Setup in Current..... | 48 |
| C. Entrainment Studies..... | 50 |
| 1. Inception of Droplet Formation..... | 50 |
| 2. Loss by Entrainment..... | 51 |
| D. Boom Geometry..... | 54 |
| 1. Boom Cross Section..... | 54 |
| 2. Three-Dimensional Effects..... | 55 |
| E. Effect of Waves on Oil Retention..... | 56 |
| 1. Setup..... | 56 |
| 2. Entrainment..... | 58 |
| 3. Boom Geometry and Response Effects... | 59 |
| F. Multiple Boom Studies..... | 60 |
| G. Absorbent - Experl..... | 62 |
| V. CONCLUSIONS..... | 63 |
| REFERENCES..... | 66 |
| APPENDIX A - EQUATIONS FOR CONTAINED SLICK LENGTH..... | 67 |
| APPENDIX B - COMPUTER PROGRAM FOR CALCULATING SLICK CHARACTERISTICS AND ENTRAINMENT LOSS RATE... | 72 |
| APPENDIX C - EXAMPLE OF LOSS CALCULATIONS..... | 75 |

LIST OF FIGURES

- Figure 1 - Typical Calculated Slick Length Showing Variation with Current, Contained Volume, and Specific Gravity
- Figure 2 - Typical Calculated Oil Thickness at the Boom Showing Variation with Current, Contained Volume, and Specific Gravity
- Figure 3 - Typical Calculated Slick Length Showing Variation with Current, Headwave Froude Number, and Interfacial Friction Coefficient
- Figure 4 - Typical Calculated Oil Thickness at the Boom Showing Current, Headwave Froude Number, and Interfacial Friction Coefficient
- Figure 5 - Calculated Minimum Slick Length Required to Prevent Entrainment Loss (Optimistic)
- Figure 6 - Calculated Minimum Slick Length Required to Prevent Entrainment Loss (Pessimistic)
- Figure 7 - Comparison of Measured and Calculated Entrainment Loss Rates
- Figure 8 - Entrainment Loss Rate as a Function of Current Speed, Contained Volume, and Specific Gravity
- Figure 9 - Maximum Theoretical Volume of Oil Contained in Calm Water
- Figure 10 - Expansion of Typical Scale Model Data for Oil Loss Rate
- Figure 11 - View of 80-Foot Towing Tank
- Figure 12 - Details of the Hinged Plate Wavemaker

Figure 13 - View of the Towing Carriage (Shown with Flat Plate Boom Model)

Figure 14 - Carriage Drive System

Figure 15 - Flat Plate Model

Figure 16 - Angled Boom Model, $\alpha = 30^\circ$

Figure 17 - Inflated Cylinder Dynamic Model

Figure 18 - Details of Inflated Cylinder Dynamic Model

Figure 19 - Two Alternate Dynamic Models

Figure 20 - Details of Two Alternate Dynamic Models

Figure 21 - Headwave Geometry

Figure 22 - Characteristic Froude Number of the Headwave

Figure 23 - Oil Slick Geometry; No. 2 Diesel Fuel, Fixed Volume
= 1.0 Ft³/Ft, Boom Depth = 5 Inches

Figure 24 - Data Showing Diesel Fuel Slick Length as a Function
of Contained Volume

Figure 25 - Diesel Fuel Slick Length as a Function of Current
Velocity Showing Comparison with Calculated Values

Figure 26 - Slick Length for Motor Oil and Fresh Water Over Salt
Water

Figure 27 - Diesel Fuel Entrainment Loss Rates

Figure 28 - 30 Weight Motor Oil Loss Rates

Figure 29 - Effect of Wave Period on Slick Setup

Figure 30 - Effect of Waves on Oil Setup

Figure 31 - Oil Setup Versus Wave Height and Period

Figure 32 - Comparison of Slick Geometry in Single and Double Boom Experiments

C-1 - Assumed Boom Geometry

C-2 - Entrainment Loss Rate in Corners

C-3 - Specific Volume and Contained Volume

LIST OF TABLES

| | Page |
|--|------|
| Table 1 - Entrainment Coefficients..... | 21 |
| Table 2 - Terminal Rise Velocity Ratios..... | 35 |
| Table 3 - Properties of Various Oil Products..... | 41 |
| Table 4 - Parameters Used to Calculate Slick Length in Figures..... | 59 |
| Table C-1 - Results of Sample Calculations..... | 79 |

I. INTRODUCTION

The hydrodynamic aspects of oil containment by retention booms were investigated for the United States Coast Guard under Contract No. DOT-CG-00504-A during the period from January to October 1970. The objectives of the study were to develop a fundamental understanding of oil retention hydrodynamics, to derive proper scaling laws and procedures for model experiments, and to provide model test data and criteria which can be used to predict containment performance of prototype booms under adverse environmental conditions.

Oil spills at sea are becoming more numerous and such spills are recognized as a major environmental hazard which must be cleaned up as rapidly as possible. A major component of many proposed clean-up systems is a containment boom. Floating oil can be herded into a confined area where its depth is great enough to allow special methods to be applied to separate the oil from the water. The floating "fence" used to "herd" the oil is generally referred to as a boom. In its simplest form the boom may be envisioned as a vertical plate having buoyancy elements so that the barrier seeks an equilibrium position at the water surface with a resulting freeboard and draft.

The mechanism by which a boom collects oil is most easily understood in two dimensions. If the boom has no relative velocity with the water or the air above the water there is no tendency for oil to thicken on either side of the barrier. However,

if there is a relative current or wind the resulting shear forces on the oil-water or oil-air interface will cause a flow of oil toward the barrier. This flow will result in a thickening of the oil on the upstream side of the barrier. The relative current required to achieve this thickening may arise from mooring the boom in natural currents or by towing the boom through the water. As the oil layer is thickened a hydrostatic pressure is built up to oppose the current forces. For a given volume of oil, current velocity and oil specific gravity an equilibrium oil thickness should be reached if there is no loss of oil past the barrier.

Actually, even in calm water (no waves) the mechanism of oil buildup ahead of the boom in a relative current is rather complex. When the velocity begins to increase, the thickness near the boom increases and this region of increased thickness propagates forward of the boom. If the terminal velocity is assumed to be reached in a relatively long time the flow may be visualized to have the following characteristics. This description assumes a fixed amount of oil exists upstream of the boom.

- 1) As the velocity is increased incrementally, the thickness of oil ahead of the boom increases and the length of the oil layer decreases. This effect of current or other forces to compress the oil layer is commonly referred to as setup.

- 2) At low velocities the oil thickness at the boom is small and the extent of oil forward of the boom is very large. Consequently the shear force on the oil-water interface acts over a large area and is the principal force causing the oil thickening at the barrier. This shear force causes the oil layer inside elevation to appear wedge shaped. The wedge has roughly a parabolic profile.
- 3) At practically all velocities, it is observed that the leading edge of the oil far upstream of the boom is shaped like one half of an arrowhead. This "headwave" is characteristic of all such density currents, and its size is determined by the relative current and the oil specific gravity. The oil thickness increases to a maximum in this leading edge region at a slope of approximately 30 degrees to the horizontal. The flow then appears to become very rough, similar to an inverted breaking wave or hydraulic jump, and the thickness almost abruptly becomes about one-half its maximum value. Clearly a drag force acts on the oil volume as a result of this leading edge action. At very low velocities and large volumes of oil this "head" force is small compared to the shear force and the oil profile or setup is characteristically a thin parabolic wedge. Typical oil profiles with moderately sized headwaves are shown in Figure 23.

- 4) As the velocity is increased the oil upstream of the boom increases in thickness and decreases in forward extent. The headwave size is proportional to the velocity squared. As a result the headwave and the turbulent action associated with it becomes a more predominant feature. In fact the drag force associated with the headwave becomes increasingly large as compared to the shear force in balancing the hydrostatic head caused by the increased oil thickness at the boom. The increased turbulent activity at the headwave is accompanied by a break-up of the oil interface in this region into droplets.
- 5) Finally a velocity will be reached for which oil escapes beneath the boom and for higher velocities the boom can rapidly lose almost all of the oil previously contained on the upstream side. This failure or maximum containment velocity may be reached by either of two mechanisms. These are referred to as "drainage" and "entrainment". An entrainment failure is said to occur when the oil droplets formed at the headwave (or by other turbulent action) and entrained into the water flow do not have adequate time to rise back to the oil layer and so are swept under the boom. Drainage

failure occurs when the extent of oil upstream of the boom is sufficient to prevent entrainment failure, but the oil thickness at the boom simply exceeds the boom draft slightly and so must escape.

Clearly, the action of waves superimposed on the flow just described complicates the picture and leads to lower maximum velocities for effective containment. Three-dimensional effects further complicate the flows associated with real oil booms.

The purpose of the experimental and analytical study reported here was to develop an understanding of these complex flows and thus to provide information necessary for the design and evaluation of oil containment booms.

The problem of oil containment was approached in a manner such that theoretical and experimental efforts were complementary. Thus, experiments were designed to test theoretical predictions. The theory was altered, in turn, to reflect experimental findings and to suggest directions for further laboratory studies. Because of the great interdependence between the experimental and analytical work carried out in this investigation, the following section (II) describes the various aspects of the study, reviews existing information, explains the analyses which were carried out and frequently refers to the experimental results which are presented in detail in later sections. Section II is therefore a summary of the various aspects of oil slick hydrodynamics based on both experimental and theoretical efforts. Equations and

curves which may be useful to the boom designer are also presented in Section II. The design curves are generally applicable to full scale booms and have been projected from model test results with corrections, where necessary, to account for model scale effects. Details of the model test equipment and procedures that were used can be found in Section III.

Substantive data and discussion of the model test results that we have used to develop the summary of hydrodynamics are presented in Section IV.

II. SUMMARY OF OIL SLICK HYDRODYNAMICS

A. The Headwave

The headwave is a characteristic phenomenon of two-phase, density-stratified flows. Headwave formations have been observed at the leading edge of: muddy water flowing in clear water (turbidity currents), salt water intrusion in fresh water, cold fronts moving into warm air, and oil slicks contained by booms against water current (see Figure 2) and Reference 9). Dimensional analysis shows that the details of stratified flows are controlled by three major non-dimensional parameters: Reynolds' number, Weber number, and Froude number. These parameters are associated with the balance between inertial and viscous forces, inertial and interfacial tension forces, and inertial and buoyant forces, respectively. In the ideal case of inviscid fluids with no interfacial tension, the flow can be characterized entirely by the densimetric Froude number:

$$P_d = \frac{U}{\sqrt{g l \frac{\Delta \rho}{\bar{\rho}}}}$$

where

U = Relative fluid velocity, ft/sec

g = Local gravitational acceleration, ft/sec²

l = A characteristic length, ft

$\Delta \rho$ = Density difference between fluids, i.e., $\rho_w - \rho_o$, lbm/ft³

$\bar{\rho}$ = Average density of fluids, lbm/ft³

For the particular case of an oil slick headwave (far upstream, so as not to be influenced by the boom), it is convenient to redefine the densimetric Froude number

$$F_d = \frac{U}{\sqrt{g(1-s)t_h}} = \frac{U}{\sqrt{g't_h}}$$

where

t_h = Maximum headwave thickness, ft

s = Specific gravity of oil $\frac{\rho_o}{\rho_w}$, and

$g' = g(1-s)$, ft/sec²

subscripts o and w refer to oil and water, respectively.

Experimental evidence with real fluids (References 1 and 9) indicate the existence of a unique headwave geometry. Thus, the shape of the headwave is fixed (see Figure 21), the ratio of headwave thickness to slick thickness t_h/t_s is fixed, and t_h is proportional to U^2/g' . The proportionality constant (F_d^2) is not known exactly. However, the headwave Froude number has generally been observed to be close to unity. Real fluid effects arising from viscous and interfacial forces can alter the size and geometry of the headwave from the ideal case. Experimental data are presented in Section IV-A. These data confirm that for a specific oil and moderate velocities the velocity and headwave thickness are related by a constant headwave Froude number of approximately one.

B. Oil Slick Setup

With ideal fluids, the profile of an oil slick contained in calm water would consist of a leading edge headwave followed by oil of uniform thickness. In reality, viscous shear forces from wind and current cause the slick to thicken downstream from a point of minimum thickness behind the headwave. Gravity waves passing through the slick create local disturbances and also affect the average distribution of oil.

1. Wind and Current

The mechanism of slick thickening (References 1, 7 and 10) in wind and current is well understood in a general sense. The oil layer thickens in order to achieve equilibrium between horizontal shear forces and buoyancy forces. A first order approximation to the differential equation governing the thickness is developed in Appendix A and shows that

$$\frac{dm}{dx} = \frac{E\tau}{g'\rho_w t} = \frac{E\tau}{g\Delta\rho t}$$

where

$\frac{dm}{dx}$ = local interfacial slope, ad

$E\tau$ = sum of shear forces at free surface and the interface, lbf/ft^2

t = local slick thickness, ft

The difficulty with using this theory lies in the great complexity involved in the shear forces. Available theories for shear forces on solid bodies are inadequate to account for such effects as interfacial capillary waves, flow separation behind the headwave, and circulation in the oil slick.

For engineering estimates the problem of slick setup can be greatly simplified by assuming that the shear forces are constant along the slick. Hence, the slick is assumed to have a parabolic thickness distribution behind the headwave. Slick setup is then easily calculated by using empirically determined shear coefficients. The greatest difficulty using this method lies in extrapolating the coefficients found from small scale model tests to full scale conditions.

Data for oil slick setup in current are presented in Section IV-B. Similar data for setup in wind are found in Reference 1. The computer program listed in Appendix B was used to find coefficients for the simplified theory that would give good agreement with experimental data. These coefficients (see Table 4) ranged from headwave Froude number $F_d = 1.0$ to 1.3 and interfacial friction coefficient $C_f = 0.002$ to 0.013.

Typical predictions of the simplified oil slick setup theory (Appendix A) are shown in Figures 1 to 4. Two-dimensional slick length and oil thickness at the boom are shown as a function of current for several values of: specific contained volume, oil specific gravity, headwave Froude number, and interfacial friction coefficient. The effects of contained volume and specific

gravity can be seen in Figures 1 and 2, while Figures 3 and 4 show the relative importance of variations in headwave Froude number F_d and interfacial friction coefficient C_f . Model test data and comparisons between data and computed slick length are presented and discussed in Section IV-B.

It should be noted that these projections for slick length and thickness may not be of practical interest over the entire ranges of parameters given. For example, the slick length of a large volume of oil in high current may be a moot point because it is not physically possible to collect and/or contain a slick under these conditions.*

2. Waves

An experimental study was conducted on the effects of combined current and waves on the setup or thickening of a contained oil slick. These tests indicated that under certain conditions there could be significant increases (up to a factor of 3) in the mean slick thickness over the current alone case. The details of the tests conducted and photographs of this phenomenon are presented in Section IV-E.1.

*A general warning is in order concerning the full scale projections presented in this section. These have been made to the best of our knowledge but it was required to make many simplifying assumptions. We do not know to what extent extrapolation of test data is justifiable. In some cases, design curves may have been extended beyond the point where realistic estimates can be made at this time.

To date it has not been possible to provide a quantitative theory for slick setup in combined current and waves. It is probable that a balance is established between the incident, reflected, and transmitted wave energy and the thickening of the slick. The mechanism by which the balance is achieved is not understood at this time. As a result, the relative importance of the boom response characteristics and slick characteristics is not clear.

At the scale of the tests, the maximum setup of the slick was accompanied by the breaking of the incident waves in the slick. In this regard, the most important parameter influencing the setup under the conditions tested was the steepness of the incident waves. These data are presented in Figure 30. Figure 31 presents these data in a dimensional form as a function of wave height and period. Large setups are seen to have occurred for the range of frequencies tested. Thus it is felt that a simple resonance phenomenon is not the responsible mechanism.

Several boom models with different response characteristics were included in the tests. In the case of a rigid barrier, with a draft that was large with respect to wave length, even steep waves were reflected with no setup resulting. However, for other boom models with varying amounts of surge, pitch, and heave stiffness and dimensions small with respect to the waves, the barrier characteristics had only minor effects on the setup.

A review of the photograph in Figure 29 indicates that the typical gravity headwave shape of the leading edge of the slick becomes more distorted with increasing setup due to waves. Thus it is unlikely that a simple superposition of velocities is responsible for the increased setup. Calculations indicate that the mass transport velocity of the waves is not large enough to cause the observed setup.

If the observed setups in combined current and waves Froude scale, as the setups in current alone do, then this phenomenon could have serious effects on full scale containment. Boom depth will have to be significantly increased to prevent catastrophic drainage failures or the current speed will have to be reduced. Thus, as a result of its possible full scale importance and lack of quantitative understanding, oil slick setup in combined waves and current must be considered a primary topic for further study.

C. Entrainment

One of the mechanisms by which oil can escape from a floating containment boom can be described as entrainment. In this type of failure oil droplets from the contained slick are entrained into the water passing under the slick and are carried beneath the boom. Based on the experimental and theoretical work conducted, a reasonable qualitative understanding of the entrainment phenomenon has been developed. However, due to its extreme complexity only limited quantitative information on entrainment is available.

1. Droplet Formation

Experimental studies indicate that the primary region in which droplets are formed and entrained into the water is just behind the headwave. There is a critical speed for any given oil at which droplets are first formed and entrained. Below this speed there is no droplet formation and above this speed the number of droplets formed and the volume of oil entrained increases rapidly. The experimental procedures and data on which these conclusions are based are presented in Sections III and IV-C.

The critical speed for droplet formation is a complex function of the interfacial tension between the oil and water and the viscosity and density of the oil. The experiments described in Section IV-C indicate that the critical speed for droplet formation is strongly influenced by the interfacial tension. The available data indicates that the critical speed varies as the interfacial tension to the $1/4$ power. The effect of variations in density and viscosity on droplet formation speed is much less than the effect of interfacial tension. A five percent increase in density and a 90 fold increase in viscosity reduced the droplet formation speed 18 percent or from 1.1 to .9 ft/sec. If it is assumed that there are no anomalous changes of the droplet formation speed within or near the range of properties tested, it may be expected that for the range of oil produced or transported by sea, the droplet formation speed will range between .8 and 1.3 ft/sec. The exact value of droplet formation speed for any given oil product will have to be determined by experiments such as those described in Section IV-C.

The quantitative analysis of entrainment losses is made much more complex by the fact that the oil droplets formed behind the headwave are of two types (see Section IV-C). These include small drops of pure oil and large oil covered water droplets which contain only a small volume of oil. The tendency to form these two types of droplets is a function of the characteristics of the oil including additives and the current speed. A much more detailed test program will be required to determine the types of oil and the conditions which result in a significant formation of oil covered water droplets.

The size of the oil droplets that are formed behind the headwave is critical in determining their rise velocity and thus the conditions under which oil will be lost. An extensive review of the literature (References 2, 3 and 4) on droplet breakup indicates that the size of the droplets will depend on interfacial tension, σ , speed, U , viscosity of the continuous fluid, ν , viscosity of the droplet, ν_o , density of the continuous fluid, ρ_w , and the density of the droplet, ρ_o . The most probable relationship for the droplet size has the form (Reference 4)

$$\text{Diameter } d = C_1 \frac{\sigma^{N_1}}{U^{N_2}} \left(1 + .7 \left(\frac{\rho_o \nu_o U}{\sigma} \right)^{.7} \right)$$

Depending on the flow conditions, three sets of values have been proposed for the constant N_1 and N_2 . They are

| | | |
|--------|-------------|-------------|
| Case 1 | $N_1 = .5$ | $N_2 = 1.$ |
| Case 2 | $N_1 = 1.0$ | $N_2 = 2.0$ |
| Case 3 | $N_1 = 1.5$ | $N_2 = 2.5$ |

The experiments described in Section IV-C indicate that case 2 or case 3 is the more likely one. Further experiments are required to confirm the correct values for a breaking headwave. For case 2 the value of C_1 for the typical droplet diameter is 7.26 and for case 3 the value for C_1 is 251.

Note: C_1 has dimension $\text{ft} \left(\frac{\text{ft}}{\text{sec}} \right)^{1/2} \left(\frac{\text{ft}}{\text{lb}} \right)^{1/2} H_1$

The relationship presented above applies only to the case of pure oil droplets. No information is presently available on the relationships which govern the size or oil content of an oil covered water droplet.

In the experiments reported in Section V-C all droplet formation was observed to take place at the aft side of the headwave or, in some cases, to a limited extent directly in front of the boom. In no cases were the interfacial waves between the headwave and the boom observed to become unstable and entrain droplets in the water. In tests with large specific volumes of diesel oil, oil covered water droplets, which were formed at the headwave, returned to the oil water interface before reaching the boom but did not coalesce. These drops were then carried aft by the flow and gave the superficial appearance that they were formed at the interface. It is believed that because of the similar test conditions, the interfacial entrainment reported by Texas A & M in the Wilson Industries design report was actually this phenomenon. Reference 1. However it is possible for higher speeds (above 1 kt) than tested and long slick lengths that droplets from interfacial waves will be entrained.

Theoretical stability criteria can only predict the speed at which the flow first becomes unstable, e.g., Kelvin-Helmholtz criterion for interfacial capillary waves:

$$U^2 = 2 \left(1 + \frac{\rho_w}{\rho_o} \right) \sqrt{\frac{\sigma}{\rho_w}}$$

The break up of interfacial waves into droplets occurs at a higher speed which must be found experimentally. It is possible that Keulegan's stability criteria (Reference 5) may yield a suitable empirical constant B:

$$B = \frac{v^2}{v_o g'}$$

2. Droplet Rise

In order for losses to occur by entrainment, the droplets must not have risen back to the interface and coalesced by the time the boom is reached. For pure oil droplets, it is realistic to assume that the droplets coalesce as soon as they reach the oil water interface. This is not true for oil covered water droplets. Thus for pure oil droplets, the velocity at which oil is lost is a function of the slick length between the boom and headwave L_h , droplet rise velocity V_r , and the rise height. It is reasonable to assume (based on observations) that droplets are entrained to a depth of 1.35 times the headwave thickness (t_h) and that the rise height is equal to the difference between the entrained depth and the depth of oil behind the headwave. The maximum velocity for which all of the oil returns to the slick is given by $U_o = \frac{V_r L_h}{1.35 t_h}$. Information on the geometry of the headwave is given in Section IV-A.

The following formulations may be used to provide a first order estimate of the droplet terminal rise velocity for the range of Reynold's numbers indicated

$$1. \text{ Newton's Law for } Re = \left(\frac{V_r d}{\nu_w} \right) > 500$$

$$V_r = 1.74 \sqrt{g'd}$$

$$2. \text{ Intermediate Law for } 2 < Re < 500$$

$$V_r = \frac{1.5(g'd)^{.71} d^{1.14}}{\nu_w^{.43}}$$

$$3. \text{ Stoke's Law for } Re < 2$$

$$V_r = \frac{g'd^2}{18\nu_w}$$

When the headwave is in the vicinity of the boom ($L_h < 3H$), the flow field of the boom aggravates the flow behind the headwave and oil loss may start at a lower speed than the critical speed mentioned above.

Based on the relationships presented above it is possible to estimate the slick length necessary to prevent entrainment of a droplet formed at the headwave for a given speed U_o . The volume and thickness of the slick at the required length may be obtained from the information in Section II-A and B.

The procedures described above to calculate minimum required slick lengths have been programmed and typical results are presented in Figures 5 and 6. Figure 5 is based on the optimistic assumption that droplet size varies as case 2 and that oil of a given specific gravity has a typical viscosity. Figure 6 is based on the pessimistic assumption that the droplet size varies as case 3 and oil of a given specific gravity has the lowest probable viscosity. The calculations indicate that for higher current speeds the more dense oils require shorter slicks than the lighter oils. This surprising result is due to the effects of viscosity. The more viscous drops are larger and as a result a point is reached when their drag coefficient is sufficiently lower than that of the smaller, lighter drops that they rise faster in spite of their greater density.

Figures 5 and 6 indicate some of the problems of trying to contain oil in currents of 2 knots. At this speed the minimum slick length to prevent entrainment of droplets from the head-wave could range from 60 ft to over 200 ft depending on the oil and assumptions made. In order to prevent drainage failure with oil of specific gravity = .95 at the required slick lengths, the barrier depth must be between 4 and 5 feet. In order to maintain these slick lengths with minimum entrainment losses, the boom must be deployed in a very deep "U" configuration or a rectangular configuration.

At speeds of 1 knot the situation is much improved in that the minimum required slick lengths decrease to between 6 and 12 feet. At speeds of about 3/4 knot, entrainment is no longer a problem in that the headwave does not break up. Bear in mind that the forgoing discussion applies only to slicks contained in calm water. The effect of waves on droplet formation is discussed in Section II-C.4.

3. Entrainment Loss

As indicated above, the development of quantitative information on entrainment loss rates presents several complex problems. The available experimental data are presented in Section IV-C. The use of these data to predict full scale entrainment loss rates requires that a number of assumptions be made. These assumptions have been made and a semi-empirical theory for entrainment loss rate is presented below. These assumptions should be regarded as tentative until more experimental data can be obtained.

In order to calculate the entrainment loss rate, the volume rate at which oil droplets are entrained from the headwave region and the volume of these droplets which escape under the boom must be determined. In Reference 6 the entrainment rate of external fluid into a headwave region of a two-dimensional gravity current in two miscible fluids is given by

$$\dot{V}_E = \beta' U_c t_h$$

where

\dot{V}_E = Entrainment rate, ft³/ft-sec

β' = Entrainment coefficient, nd

U_c = Current speed, ft/sec

t_h = Headwave thickness, ft

The first assumption made is that this type of equation can be applied to the case of a two-dimensional gravity current in immiscible fluids in which entrainment is by droplet formation. The entrainment coefficient β' can be estimated from entrainment data for the case when the headwave region is close enough to the boom that all droplets formed can be taken to have been lost under the boom. Table 1 presents the values of β' deduced from the data in Section IV-C.2.

TABLE 1

Entrainment Coefficients

| U_c ft/sec | β' | Specific Gravity | Interfacial Tension dynes/cm |
|--------------------------------|----------------|---------------------|---------------------------------|
| 1.14 | .00715 F_d^2 | .86 | 1 |
| 1.44 | .00748 F_d^2 | .86 | 16 |
| 1.23 | .00574 F_d^2 | .86 | 16 |
| 1.08 | .00465 F_d^2 | .906 | 18.8 |
| F_d = Headwave Froude Number | | | |

The entrainment coefficients in Table 1 apply only to the case of pure oil droplets. It should also be noted that this coefficient, β' , may also be a complex function of oil properties such as interfacial tension, viscosity and density. No information is available on the effects of these properties on β' .

The rate at which droplets, which have been entrained, escape under the boom can be estimated if it assumed that any droplets which have not risen back to the slick by the time the boom is reached are lost. This is not strictly true but it is a good first approximation and is conservative. Information on minimum droplet size and rise velocity are presented in Sections II-C.1 and II-C.2 above. Although no detailed measurements have been made, observations suggest that the largest pure oil droplets are about 4 times the diameter of the smallest. It has also been assumed that the distribution of volume between the largest and smallest droplets is uniform. This assumption should be checked experimentally.

Based on the above analysis a computer program was written to calculate entrainment loss rates as a function of current speed, oil volume and oil properties. This program is described in Appendix B. A comparison between calculated and measured entrainment loss rates is presented in Figure 7. Considering the many assumptions and simplifications in the theory, the agreement is satisfactory.

In order to determine the importance of entrainment loss under full scale conditions, a series of parametric calculations were carried out. The results are presented in Figure 8. Although the loss rate per second per foot of boom may seem small, for realistic boom lengths and times the loss could be unacceptable. For example, in a current of 2 ft/sec a 1000-ft boom containing 10,000 ft³ (about 250 tons) of oil of .85 specific gravity and distributed uniformly along the boom, oil will be lost at a rate of 1×10^{-3} ft³ per sec per foot of boom. This amounts to a total loss of 1 ft³ per second or 3600 ft³ per hour if the total volume is maintained. Thus, it may be concluded that entrainment losses will be important and can best be controlled by maintaining low current velocities and long slick lengths. A more detailed example is presented in Appendix C.

9. Effect of Waves on Entrainment Loss

An analysis and prediction of the quantitative effects of waves on the entrainment loss rate past a floating boom is an extremely complex problem. As a result, qualitative and quantitative projections of the effect of waves on entrainment must be largely based on the limited experimental observations available. These experimental observations are reported in Section IV-E and indicate that there are three sources of entrainment loss in waves. These sources are summarized below.

(1) Headwave Effects

The wave orbital velocities tend to superimpose on the current velocities at the wave crests and cause an increase in the headwave entrainment. Effective additions to the

current velocity of from 20 to 70 percent were noted (see Section IV-E.2) in shallow waves, i.e., $\frac{u}{\lambda} < 0.04$.

A quantitative estimate of the importance of this effect can be derived from the information in Figures 5 and 6. In a current of one knot and a 5 ft. wave with a 5 sec. period the effective current at the headwave may be on the order of 3.5 ft/sec. Using Figure 5 and calculating backward for a $SG = .85$, the rise velocity of the smallest drop will be about .066 ft/sec and it will have to rise about 1.41 ft. The average current sweeping it aft is one knot which will require a slick length of about 35 feet to prevent loss. This compares with a slick length of 5.4 ft for a one knot current in calm water.

In the event the slick is short enough so that most of the entrained droplets escape, it may be expected that the loss rate will approach the asymptotic loss rate indicated in Figure 8 for the value of the effective current. It is likely that the value of the entrainment coefficient, β' , will be affected by the increased turbulence in waves and as a result the use of information from Figure 8 must be regarded with caution. There are no experimental data available at this time on the effect of waves on β' .

(2) Breaking Waves

Steep waves that enter a slick may steepen further and break. The resulting turbulence results in the formation and entrainment of droplets at the interface. No quantitative

information on the entrainment loss rate from this source is available. It is probable that this type of entrainment is most serious under the same wave conditions which cause large setup of the slick. This phenomenon was discussed in Section II-B.2.

(3) Near Boom Entrainment

Entrainment losses can occur from the region of a slick near the boom when there are large relative motions between the boom and the surrounding fluid. Relative motions in the horizontal plane are much more serious in this regard than motions in the vertical plane. The worst near boom entrainment observed in the model tests (see Section IV-B.3) occurred in the case of a boom concept which was restrained in surge but free in pitch. The resulting pitch motions from the surge-pitch coupling resulted in large alternating relative velocities at the lower edge of the boom. The "starting" vortices which were formed under the boom entrained oil from the slick. Restraining the boom in pitch with a towing bridle greatly reduce the pitch motions and, thus, the entrainment losses. The smallest relative motions in the horizontal plane were obtained when the boom models were given compliance in surge and were restrained in pitch. Limited quantitative information concerning conditions under which losses due to near boom effects will occur is discussed in Section IV-B.3.

Heave relative motions were not significant for near boom entrainment except in the case of large discontinuous changes in the waterplane area. When such a boom heaves somewhat out of phase with the waves, the resulting agitation drives oil droplets down into the water column where they are swept under the boom.

D. Drainage

The simplified theory for slick setup in calm water can be readily used to predict the maximum volume of oil that can be contained by a boom in current. The assumption is made that a particular specific volume is contained if the boom draft $H \approx t/s$, where t is the slick thickness at the boom and s the oil specific gravity. Any oil in excess of the maximum volume is lost by drainage under the boom. The equations given in Appendix A for setup are used to develop the following expression for maximum nondimensional volume.

$$\frac{V}{H^3} = \frac{\left(\frac{1}{s}\right)^3 - 0.216 \left(\frac{P_H}{P_d}\right)^3}{\frac{3}{2} \frac{C_F}{s} P_H^2} + 5.64 \left(\frac{P_H}{P_d}\right)^3$$

where

V = Specific volume, ft^3/ft

H = Boom draft, ft

F_H = Boom Froude Number $U/\sqrt{g'H}$

F_d = Headwave Froude Number

C_f = Interfacial friction coefficient

Typical curves from this equation are shown in Figure 9.

The curves are straight lines when the boom Froude number F_H is less than 0.6 and 0.9 for $F_d = 1.0$ and 1.4, respectively. The slope is just -2.0. Thus, for low values of F_H the maximum non-dimensional contained oil volume is proportional to $1/F_H^2$, so for a particular oil, the maximum specific volume that can be contained is proportional to H^3/U^3 . If a maximum volume of oil were contained in some current and then the current was increased ten percent, about 20 percent of the volume would be lost by drainage establishing a new equilibrium condition.

The maximum boom Froude number for which oil theoretically can be contained corresponds to $\sqrt{H^3} \approx 15$, i.e., when the oil volume is just equal to the headwave volume and the boom draft is equal to the minimum oil depth behind the headwave. This is an unstable condition; any disturbance will cause the entire volume to drain under the boom. For small volumes, $\sqrt{H^3} < 15$ the headwave is influenced by the boom's flow field at high boom Froude numbers. Experiments indicate that in this region the limiting current at which the oil can be contained before complete drainage failure occurs can be approximated by $F_H = F_d$.

No model tests were made in this program to check the theoretical predictions of maximum volume that can be contained for large values of V/H^3 . However, data presented in Robbins' Thesis, Reference 7, for No. 2 Diesel Fuel show good agreement with the theory for a value of $C_p \approx 0.005$. Unfortunately, these data were obtained from very small scale tests at low current speeds.

It should be noted that local thinning of the slick that is normally observed just ahead of the boom (see photographs in Figure 23) does not occur when the oil depth at the boom is equal to the boom depth. This thinning is associated with the separated region below the slick and ahead of the boom. The size of this eddy is roughly proportional to the depth of the boom extending below the oil slick. As the oil depth increases at the boom, the eddy becomes smaller and finally disappears when the oil depth is equal to the boom draft.

The effect of waves on drainage is closely related to slick setup in waves which was discussed in Section II-B.2.

A simple approach to the design of boom draft to prevent drainage in waves is to let

$$H = t \cdot \frac{t}{t_c} \cdot a$$

where

H = boom draft

t = slick thickness at boom in calm water

$\frac{t_w}{t_c}$ = wave setup factor (see Section IV-E.1 and Figure 30)

α = a factor which accounts for relative heave motion of the boom with respect to the interface

E. Scale Model Testing

In order to evaluate and refine the characteristics of an oil boom design, it would be desirable to be able to conduct true scale model tests. The feasibility of conducting such model tests has been investigated and the testing procedures developed to the extent possible within the limitations of the scaling parameters.

1. Scaling Parameters

In conducting a scale model test it is necessary to identify the physical characteristics of the system which are important. These characteristics are then sorted into dimensionless groups on the basis of theoretical considerations or dimensional analysis. In the test program the results are derived as a function of the important dimensionless groups. The limitation of this procedure is that results may be a function of several dimensionless groups which cannot be satisfied simultaneously.

The drainage mode of failure is directly related to the thickening of the slick in front of the boom. The slick is a typical gravity current which is characterized by a headwave which grows to about twice the mean thickness of the slick aft of the headwave. When inertia and gravity dominate, the speed of propagation of the slick can be defined by a Froude number.

The fact that headwave and slick propagate at a constant Froude number suggests that a critical speed for drainage failure should be defined on the basis of a critical Froude number based on boom depth. The tests to date indicate that this failure criterion is so. If the volume is very large, the slick aft of the headwave will tend to thicken due to interfacial stresses. This will tend to reduce the critical Froude number for drainage. Estimates of this effect have been made and are reported in Section II-D.

The other mode of failure is much more difficult to model because it involves the entrainment of droplets under the boom. In order to model the entrainment of droplets the following items must be modeled:

1. The basic flow field around the slick and boom,
2. The formation of the droplets,
3. The rise of the droplets back to the slick or entrainment under the boom.

The basic configuration of the slick and the flow field around the slick and boom will be modeled if the Froude number is maintained and geometrically similar booms and volumes of oil are used.

The scaling of the formation, size, and volume of droplets off the aft end of the headwave is critical. For a given oil, the test results show that the headwave breaks and forms droplets at a fixed speed so long as the headwave is not in the boom's flow field, i.e., is greater than three boom drafts ahead of the boom. This is consistent with the hypothesis that the formation and size of the droplets is a function of the dynamic pressure forces tending to cause break up and the surface tension forces resisting break up. This results in a form of the Weber number being an important non-dimensional parameter. The form of the Weber number is given by

$$\text{Weber Number} = \frac{U_{cr}}{\left(\frac{\sigma \frac{\Delta \rho}{\rho_w} g}{\rho_w} \right)^{\frac{1}{2}}}$$

where

U_{cr} = Speed for inception of droplet formation at aft end of headwave,

σ = Interfacial tension,

-32-

g = Gravitation acceleration constant,

ρ_w = Density of water, and

$\Delta\rho$ = Density difference between oil and water.

The critical speed may be a function of parameters such as the density ratio and viscosity ratio between the oil and water. These can be modeled by using the same oil in the model as full scale. When the interfacial tension is reduced to maintain the proper Weber number in a model, a complicating factor may be the ratio of the viscous restoring forces to the surface tension restoring forces expressed by the parameter

$$\frac{\mu_o}{\sqrt{\rho_o \sigma D}}$$

where

μ_o = Viscosity of oil,

ρ_o = Density of oil,

σ = Interfacial tension, and

D = Characteristic dimension such as droplet diameter.

Reference 3 indicates where this parameter exceeds 0.2 the maximum droplet size will significantly increase. Calculations indicate that with diesel oil the interfacial tension may be reduced by a factor of 16 and the droplet diameter by a factor of 4 for typical droplet sizes without exceeding a value of 0.2. There could be a problem with droplet sizes, however, if interfacial tensions are reduced in oils with viscosities one order of magnitude greater than diesel oil.

The scaling of the rise of the oil droplets back to the slick after they are formed requires that the slick lengths be geometrically similar between model and full size and the ratio of droplet terminal rise velocity to current speed be maintained. If real fluid effects are unimportant Froude number scaling will result in geometrically similar slick lengths. The droplet diameter is in theory correctly scaled by scaling the Weber number. However, the droplet terminal rise velocity is a function of the droplet diameter and the drag coefficient. The drag coefficient is a function of Reynolds number based on the drop diameter, velocity and viscosity of the water. The Reynolds number can be maintained only if the viscosity of the water can be reduced. This is not possible.

It is of interest to consider the possible error in terminal rise velocity due to the error in the drag coefficient. Table 2 presents a summary for the case in which a 4:1 scale ratio has been obtained by reducing the interfacial tension by a factor of

16. Depending on the full scale droplet diameter the terminal rise velocity ratio can range from 30 percent too high to 35 percent too low. The actual full size droplet diameter distribution is not known so that it is not possible to be certain if the model test results for loss due to entrainment are conservative or optimistic. It is our impression that for the full size case referred to in Table 2 that droplet sizes in the range of 0.1 to 0.2 inches will predominate. If this is the case then the model results will be conservative. Some compensation for this effect may be possible in the test program by increasing the volume of oil in front of the boom. This will increase the slick length and allow the droplets, which rise too slowly, more time to return to the slick.

In summary, in conducting scale model tests of oil retention booms using oil, it is vital to scale both the Froude number and Weber number of the flow. Even when this is done there will be some scaling error due to Reynolds number effects on the rise velocity of the oil droplets. As a result, it is expected that the model test results will be conservative. The extent to which they are conservative cannot be estimated at this time.

TABLE 2
Terminal Rise Velocity Ratios
Scale Ratio = 4:1 in Diesel Oil

| Full Size (20" Boom) | | | | Model (5" Boom) | | | |
|----------------------|-----------|-----------|-------------|-----------------|-----------|-----------|------------|
| Current Speed | Drop Dia. | V_r fps | V_r/U_c | Current Speed | Drop Dia. | V_r fps | V_r/U_c |
| U_c | .4" | .438 | .438/ U_c | .5 U_c | .1" | .28 | .56/ U_c |
| U_c | .2" | .395 | .395/ U_c | .5 U_c | .05" | .17 | .34/ U_c |
| U_c | .1" | .245 | .245/ U_c | .5 U_c | .025" | .08 | .16/ U_c |

| Full Size Drop Dia. | $\left(\frac{V_r}{U_c}\right)_{\text{model}} / \left(\frac{V_r}{U_c}\right)_{\text{full}}$ |
|---------------------|--|
| .4" | 1.28 |
| .2" | .86 |
| .1" | .65 |

2. Expansion of Typical Model Test Data

This section presents an example of the expansion of model tests data to full scale using the principles described above. A series of tests were conducted using Diesel oil with a specific gravity of 0.86. In these tests a fixed volume of oil was contained in front of the boom over a range of speeds. The amount of oil lost in a fixed length of run was measured. All tests

were conducted at the same ratio of boom depth to water depth. Within the limits of the test facility the scale ratio was changed as much as possible. The Weber number was altered by reducing the interfacial tension by the addition of one percent by weight of the surface active agent Zonyl A. It was determined that the interfacial tension was reduced by a factor of 16 by this procedure. In maintaining both Froude number and Weber number constant this reduction in surface tension is equivalent to an increase in velocity by a factor of 2 and scale ratio by a factor of 4. Thus, a 5" model boom scales 20" boom when the interfacial tension is reduced by a factor of 16.

The experimental data for entrainment loss rate with reduced interfacial tension are presented in Figure 27. These data have been expanded to full scale and the results are presented in Figure 10. In scaling up these data the reduction in interfacial tension by a factor of 16 results in a linear scale ratio, λ , of 4. This means that the prototype contained volume in λ^3 or 64 times the model volume, the prototype speed is $\sqrt{\lambda}$ or 2 times the model speed and the loss rate is $\lambda^{3/2}$ or 8 times the model loss rate. Figure 10 also presents the calculated entrainment loss rate based on the theory presented in Section II-C.3. There is reasonable agreement between the theory and the scale model data.

3. Conclusions with Respect to Scale Model Tests

(1) In conducting scale model tests of oil booms with oil it is necessary to scale both the Froude number and Weber number of the flow. Even when the Froude number and Weber

number are scaled, uncertainties in the scaled entrainment exist because Reynolds number effects result in droplet rise velocities which may be in error.

(2) The need to scale Weber number places a limit on the scale ratio that can be applied because of the limit to which interfacial tension can be reduced. With the surface active agents used so far, the interfacial tension can be reduced by a factor between 10 and 20. This limits the maximum scale ratio to between about 3 and 4.5.

III. MODEL TEST EQUIPMENT AND PROCEDURES

A. Equipment

Sixteen-Foot Tank - Oil dynamics studies were begun in a small 2 x 2 x 16 ft. towing tank having clear plastic sides. Valuable experience was gained from tests in this facility along with some meaningful data. However, the relatively short length of this tank did not allow studies to be made on steady flows. To attain reasonable towing speeds the model was rapidly accelerated. The high acceleration produced transient flow conditions which were not completely damped out during the course of the short run. The short length also caused tests in this facility to be limited to small oil volumes. Thus, most data presented in this report were obtained from a larger eighty-foot tank described in the following section.

Eighty-Foot Tank - The tank measures 2 x 2 x 20 ft and one side is made of clear plastic sheet for viewing. The opposite side and bottom are plywood and painted white. The tank is shown in Figure 11. Water depth in the tank was normally 20 in. and reduced to 16 in. for waves.

The wavemaker is a hinged plate at one end of the tank. The plate is oscillated by a throw rod. Wave height is varied by changing the throw of an eccentric. Power is supplied by a 1/4 HP Graham variable speed drive allowing wave frequencies from 0.0 to 2.0 cps. Details of this system are shown in Figure 12. The maximum allowable wave height (for 16 in. water depth) is 3.5 in. for waves with a period, $T = 0.75$ seconds. Lower frequency waves have lower maximum heights because of throw limitations and higher frequency wave heights are limited by splashing between the wave plate and the tank end.

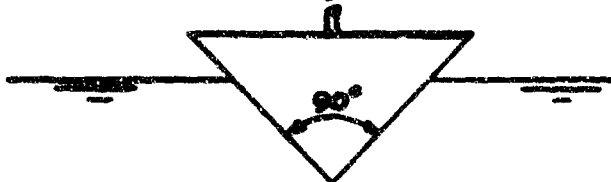
A blower was installed along with the wavemaker to produce wind generated waves. However, tests in wind generated waves were not conducted in this study since data are available in Reference 1.

A rubber tired carriage rides on steel rails along the tops of the side walls. Power is supplied by a 1/2 HP Graham variable speed drive through a pulley system with a wire towing cable. Details of the carriage and drive system are shown in Figures 13 and 14, respectively. Maximum carriage speed is about 3 fps. Speed can be maintained within ± 2 percent accuracy.

B. Models

Flat Plates - Most calm water tests were conducted using a simple aluminum flat plate suspended from the carriage as shown in Figure 13. Boom draft, H , (to 8 in.) is readily controlled in this manner. Soft rubber wipers are used to seal the small gap ($1/8$ in.) between the tank walls and the model edges. These help to assure that flow past the model is two-dimensional. A second flat plate, shown in Figure 15, was used along with the first in double boom tests.

Wedge - A 90° wedge (see sketch below) was tested in calm water to determine effects of boom cross-section geometry on oil retention ability. This model is suspended in the same manner as the flat plate and has rubber wipers also.



Angled Booms - Angled booms were tested to investigate three-dimensional (3D) effects, i.e., effects of tangential flow components. Two models, $\alpha = 30^\circ$ and $\alpha = 60^\circ$, were tested for one boom draft ($H = 5$ in.). The boom angle α , is, defined as the angle between the current direction and a line normal to the boom. Thus the normal flow case (2D) is, $\alpha = 0^\circ$. Figure 16 shows one of the angled booms used.

Dynamic Models - Tests in waves were conducted using dynamic boom models free to heave, pitch and sway in response to the seaway. The first model was designed to simulate a weighted skirt supported by an inflated cylinder. This inflated cylinder model

is shown in Figure 17, and particulars are given in Figure 18. The model was towed using a bridle and elastic line. Sway response was varied by changing the spring constant of the towline. This model was also towed in a condition where roll and sway were constrained allowing only heave motions.

Two additional models were constructed and used for dynamic tests to investigate the effect of boom geometry on oil containment in waves. Model A-1 represents an inflated rhomboidal boom in which the lower section is ballasted with sea water. Model A-2 is a simple skirt type boom with continuous rectangular flotation elements. These models are shown in Figure 19 and particulars are given in Figure 20.

All of the dynamic models are 23.5 in. long and have no wipers at the sides because they would tend to affect the models' motions. Thus, oil can leak through the 1/4 in. spaces between the model and the tank walls.

C. Properties of Test Materials

Oils - The majority of tests were made using No. 2 Diesel Fuel. Several other oil products were used in tests to determine the effects of oil properties, namely specific gravity and viscosity, on oil retention dynamics. The products that were used are listed in Table 3.

Additives - A sorbent, Ekoperl, and a surface active agent, Zonyl A, were added to oil to study their effects on retention dynamics. Ekoperl, an expanded aluminum silicate produced by Pennsylvania Perlite Corp., is reported to absorb five times its

HYDRONAUTICS, Incorporated

-41-

weight in oil (Reference 11). Zonyl A is effective for reducing the interfacial tension (IFT) between two immiscible liquids. Data from the manufacturer, DuPont, are shown in the following table for Heptane over water.

| Concentration of Zonyl A added to water (Wt. % in water) | Interfacial tension 78F (Dynes/cm) |
|--|------------------------------------|
| 0.1 | <1.0 |
| 0.01 | 10.2 |
| 0.001 | 21.3 |
| 0.0 (Control) | 48.8 |

TABLE 3
Properties of Various Oil Products

| Product | Specific Gravity, $s = \frac{\rho_o}{\rho_w} @ 60F, nd$ | Kinematic Viscosity @ 60F, cs |
|--|--|----------------------------------|
| #2 Diesel Fuel | 0.860 | 4.3 |
| (Esso) Faxon 35 | 0.883 | 19 |
| (Esso) Faxon 50 | 0.900 | 100 |
| (Humble Oil) Nuso 38 | 0.954 | 118 |
| (Wards Riverside Additive Free Motor Oil) SAE 30 | 0.906 | 380 |

Additional tests to determine effects of IFT were conducted with a thin layer of fresh water (slick) over salt water. In this case, the IFT is virtually zero.

D. Procedures

Calm Water - Tests in calm water were conducted using two different methods: continuous slick and constant volume. In the continuous slick method the oil is distributed uniformly over the entire length of the tank prior to making a run. Hence, the volume of contained oil (defined as oil between the moving head-wave and the boom) generally increases during the run. A steady state is achieved only when the flow of oil under the boom is just equal in volume to the flow entering the headwave, i.e., the volume of contained oil is constant.

In the constant volume method all of the oil is collected and contained (at about 2 in. depth) in a small area ahead of the boom by a cofferdam. The cofferdam is removed just when the boom acceleration begins. Steady state is achieved after the desired carriage velocity is reached and the oil slick has adjusted to a constant length (between the boom and leading edge of the slick). When the oil losses under the boom are large (high speed), the slick length continues to decrease and no steady condition is achieved.

Boom acceleration in the small 16-foot tank is large. The steady run velocity is attained before one foot of travel. In the larger 80-ft tank the boom acceleration is less than 0.1 ft per second and the run velocities are attained between 10 and 20 ft of travel.

Waves - Tests in waves were generally made using the constant volume method. The wave generator is started after the boom has started its acceleration. Thus, the contained oil slick and boom do not run into waves until after about 40 ft of boom travel in calm water. In this manner, observations are made before waves reflected from the end of the tank return toward the waveraker and form a standing wave pattern. A beach was installed at the end of the tank to damp out the waves, but was only about 70 percent effective for long waves ($\lambda \approx 5$ ft) and took up several feet of available run length and so was removed.

E. Observations

Slick Length - Slick length was measured by marking the position of the leading edge of the slick on the side of the tank when the boom was at a known location. Measurements were generally repeated for every 10 ft of boom travel.

Interfacial Waves - The minimum speed for the inception of interfacial capillary waves was determined by observation.

Entrainment - The region behind the leadwave was observed to find the minimum speed at which droplets of oil are formed. In many cases large oil covered water droplets or oily droplets are also seen. Individual droplets can be visually traced to determine whether they return to the oil slick or are lost under the boom.

Lost Volumes - When oil losses under the boom were significant from heavy entrainment or drainage, the volume (lost) behind the boom was collected and measured at the end of the run.

Motion Pictures - Sixteen-millimeter motion pictures were made and studied for slick geometry, headwave celerity, formation of droplets and droplet trajectories.

IV. DISCUSSION OF TEST RESULTS

A. Studies of Headwave Geometry and Propagation

Experimental evidence indicates that there is a characteristic headwave geometry for dynamic equilibrium at the leading edge of an oil slick in current. The geometry is not unique and can be altered somewhat by viscous effects, surface tension, nearfield boom effects (for small specific oil volumes), and waves. The characteristic two-dimensional headwave geometry is shown in Figure 21 where the coordinates are non-dimensionalized by the maximum headwave thickness t_h . It is seen in this figure that the minimum thickness behind the headwave t_1 is nominally $0.6 t_h$ and the length of the headwave l_h is about $7.5 t_h$.

Data showing the characteristic headwave Froude number are presented in Figure 22. Here the size parameter is taken as the maximum headwave thickness, t_h , i.e., $F_d = U/\sqrt{g' t_h}$ where $g' = g \frac{\Delta \rho}{\rho_w} = g(1-s)$. All of the data are for Diesel fuel and fresh water. Test variables were boom speed U , interfacial tension σ , and specific oil volume or thickness.

Data were taken for the boom moving into a uniformly distributed slick ($t_o > 0$) and with a fixed volume of oil ahead of the boom ($t_o = 0$). In the latter case, steady state is obtained since the headwave speed is just equal to the boom speed, $U = U_b$. With a uniformly distributed slick the headwave speed is greater than the boom speed since the volume of oil collected (between the headwave and the boom) is constantly increasing. Toward the end of a run in a distributed slick the difference between headwave speed and boom speed becomes small, the headwave thickness becomes nearly constant, and thus, a quasi-steady condition is reached.

The data from distributed slick tests show that headwave Froude number tends to decrease with increasing slick thickness. This effect can be attributed to "drag" associated with the change in momentum of oil that is collected at the leading edge of the headwave. Thus, a headwave of given size (t_h) travels slower into a slick than into clear water. If oil were withdrawn, at the boom, from the collected volume at the same rate that it is ingested by the headwave, we may expect the momentum of inflow to be balanced by the outflow momentum so that headwave celerity (and hence, F_d) would be the same as for the fixed volume tests. The headwave Froude number for the thinnest distributed slick ($t_o = 0.028$ inch) was quite close to that for fixed volume tests, $F_o = 1.2$.

Reduced interfacial tension (IPT) was shown to reduce the headwave celerity. The IPT was reduced by adding a surface active agent to the oil phase. It was not possible to accurately measure

the reduced IFT, but laboratory measurements indicated that it was less than or equal to one dyne per centimeter. With reduced IFT the Froude number defining headwave celerity was about $F_d = 1.0$. The interfacial tension tends to reduce the thickness of the headwave at a given speed. In fact, at low speeds $U < 0.5$ fps no headwaves were observed except when the IFT was reduced. Here, the inertial forces were small enough that they were balanced by the normal IFT forces. With reduced IFT, buoyancy forces were needed to provide the necessary balance, hence the observed headwave.

The Weber number is associated with the relationship between inertial forces and surface (IFT) forces as Froude number is associated with inertial and gravity (buoyancy) forces. The normal form of Weber number is:

$$We = \frac{\rho U^2 d}{\sigma} \text{ (non-dimensional)}$$

where

ρ = Fluid density

U = Velocity

d = Characteristic length

σ = Interfacial tension, IFT

It is convenient to multiply this number by the Froude number squared, using $\sigma = t_h$, to get:

-47-

$$\text{WeF}_d^2 = \frac{\rho U^4}{g' \sigma}$$

Thus, for inviscid fluids, dynamic similitude would be assured when both Froude number and Weber number are held constant and implies that with ρ and g' constant the Froude number will be constant if U^4/σ is maintained constant.

The effect of viscosity on the headwave Froude number was also investigated by tests with SAE 30 weight motor oil. At headwave speeds around one foot per second the headwave Froude number averaged about $F_d = 0.95$. Thus, increased viscosity apparently causes the headwave to have greater thickness at a given speed.

Much of the scatter in the data shown in Figure 22 results from inaccuracy in the measurement of headwave thickness. The headwave is generally not smooth as seen in the photographs in Figure 23. Interfacial instabilities arising from viscous shear forces cause interfacial waves to grow along the headwave. These waves tend to break into droplets behind the point of maximum headwave thickness. The photographs show that the slick thickness tends to increase downstream but there is a noticeable thinning just ahead of the boom. This thinning is typical and is associated with the stagnation pressures in the flow at the boom.

B. Oil Slick Setup in Current

The profile of an oil slick contained by a boom against a current is a complex function of the volume of oil, current velocity, and oil properties such as specific gravity and viscosity. The length of the slick increases with volume and decreased with current velocity as shown by the experimental data in Figure 24. Diesel oil slick lengths are shown here as a function of specific volume for several values of current velocity. A cross plot of these data is presented in Figure 25. Slick length data for 30 weight motor oil are presented in Figure 26 along with data from an experiment with a fresh water "slick" on salt water.

The slick lengths in Figures 25 and 26 can be computed by the simplified mathematical model given in Appendix B. A satisfactory fit to each set of data is obtained by varying the head-wave Froude number and the interfacial friction coefficient as required. These values are given in Table 4. The calculated slick lengths are plotted with dashed lines in the Figures. (Note: the calculated lengths in Figure 26 for 1.1 ft³/ft fresh water and 0.55 ft³/ft SAE 30 Motor oil were nearly identical, and are shown by one line.)

The calculated slick lengths are affected mostly by the value of C_f at low velocities $U < .5$ fps and by the value of F_d at high velocities $U > .5$ fps. The Froude numbers in Table 3 all fall within the experimental range for headwaves. Of course, less is

known about the interfacial shear stresses which tend to cause the slick to thicken downstream of the headwave. The values of friction coefficient C_f in the table are just convenient engineering estimators which serve to calculate slick geometry in an approximate mathematical model. No account is made for the effect of circulation in the oil slick, oil viscosity, interfacial waves, and other factors which must have a real effect on the interfacial shears.

TABLE 4
Parameters Used to Calculate Slick
Lengths in Figures 25 and 26

| | Φ , ft ³ /ft | Headwave Froude No. F_d | Interfacial Friction Coefficient C_f |
|--------------------------------|------------------------------|---------------------------------|---|
| Diesel Fuel | .50 | 1.30 | .003 |
| SG = 0.860 | 1.00 | 1.25 | .002 |
| | 2.00 | 1.12 | .002 |
| | 3.00 | 1.05 | .002 |
| SAE 30 Motor Oil | .37 | 1.09 | .009 |
| SG = 0.906 | .55 | 1.03 | .007 |
| Fresh Water Over Salt Water | 1.10 | 1.10 | .013 |
| SG = 0.959 | | | |

C. Entrainment Studies

1. Inception of Droplet Formation

Model tests show that containment booms can lose oil when droplets are formed which are entrained in the water flow beneath the boom. Major droplet formation takes place in the region just behind the point of maximum headwave thickness. Two types of droplets have been observed: 1) small pure oil droplets and 2) large oil covered water droplets or "oily" droplets which contain only very small oil volumes despite their large appearance. Both types occur regularly with Diesel fuel, whereas the 30 weight motor oil generally formed only pure oil droplets. The oily water droplets with Diesel fuel were more prevalent at higher current speeds.

There appears to be a critical velocity for any particular oil product at which droplets are first entrained into the water behind the headwave. Below this inception speed there is no droplet formation. As speed is increased beyond the inception point, droplet numbers and the entrained oil volume rapidly increase. The critical velocities for the Diesel Fuel and 30 Weight Motor Oil were found to be 1.1 and 0.9 fps, respectively. When interfacial tension was reduced by adding a surface active agent the critical speeds were reduced to 0.6 and 0.6 fps, respectively. (The respective changes in IPT were 16 to 1 and 18.8 to 12.8 dynes per centimeter.) The inception speed for any other product must be a complicated function of viscosity, specific gravity, and interfacial tension.

When the volume of contained oil is sufficiently small so that the headwave is near the boom, the speed for inception of droplets is reduced by about five percent.

2. Loss by Entrainment

The rate at which oil is lost beneath the boom by droplet entrainment is a complex function of current velocity, contained oil volume, boom draft, and oil characteristics. An oil droplet entrained into the flow at the headwave may either return to the slick further downstream or remain entrained in the flow underneath the boom. The probability of a droplet returning to the slick depends on the ratio of droplet rise velocity to current speed, and the length of the slick between the point of droplet formation and the boom.

The region behind the headwave where droplets are formed is highly turbulent. Some droplets are entrained more deeply into the water and have a greater probability of remaining entrained in the flow beneath the boom. There are always some droplets entrained nearer to the interface which are able to return to the slick. Increasing the slick length allows droplets a greater time to rise back to the slick, thus decreasing their probability of being lost. Current velocity has the greatest effect on the rate of entrainment loss. Increasing velocity causes greater volumes of oil to be formed into droplets, and the droplets are entrained more deeply into the flow. The entrained droplets are less likely to return to the slick because they have shallower trajectories and the slick length is shorter.

There is a stagnation streamline at the boom which is affected by boom geometry and depth, and the oil slick geometry near the boom. Any entrained droplet which is below this streamline as it nears the boom will be drawn under the boom. Droplets above this streamline are caught up in the separated eddy where they may be returned to the slick or be rejected back into the flow and ultimately lost beneath the boom.

Oil-water droplets in Diesel oil with high IFT were sometimes seen to return to the slick interface but did not coalesce into the slick. They were carried back along the interface towards the eddy region where some became re-entrained into the flow and were lost beneath the boom. The oil volume lost in this manner was extremely small.

Experimental entrainment loss rate data are presented in Figure 27 and 28 for Diesel fuel and 30 weight motor oil, respectively. The average rates of volume loss \dot{V}_L were obtained by measuring the volume lost during a 50 foot run. This volume is divided by the time in the run to give the average loss rate. The specific volumes listed in the figures refer to the volume contained at the start of the run. In some cases of high loss rates and small initial volumes, up to 90 percent of the "contained" volume was lost in the course of the run. The loss rate was fairly constant during runs where entrainment was relatively light, $\dot{V}_L < 10^{-3}$ ft³/ft-sec. In runs with heavy entrainment, $\dot{V}_L > 10^{-3}$, the rate tended to increase as the run progressed and the contained volume became smaller.

The solid data points in Figures 27 and 28 represent runs in which oil was lost by a combination of entrainment and drainage type failure. Runs in which oil is lost only by entrainment are represented by open symbols.

The data show that increasing the contained volume decreases the oil loss rate at a fixed current. On the other hand, increasing the contained volume allows an increase in current velocity with no increase in loss rate. For example, the current for "moderate" loss rate (defined arbitrarily as $\dot{V}_L = 10^{-3}$) can be increased eight percent by increasing the specific volume contained by a five inch flat plate boom from 0.37 to 0.95 ft³/ft. Similarly, increasing the boom depth decreases the oil loss rate at a fixed current. The current for moderate entrainment was increased ten percent when boom depth was increased from 2 to 5 inches and specific volume = 0.37 ft³/ft.

The importance of interfacial tension on the formation and entrainment of oil droplets is shown in these figures. A sixteen-fold decrease in IFT of Diesel fuel caused moderate entrainment loss rates at current velocities reduced by about 20 percent. A somewhat less substantial decrease in IFT obtained with the motor oil showed a similar tendency for increased entrainment loss rates.

Note that the maximum loss rate shown for 0.13 ft³/ft Diesel oil is less than for 0.20 ft³/ft at about 1.33 fps current. This is caused by the depletion of the smaller contained volume by

entrainment and drainage early in the run. The loss rate was substantially reduced over the remainder of the run and resulted in a smaller average loss rate.

If the curves in the figures were extended downward, they should all become straight vertical lines representing the maximum current for which there is no entrainment loss. The value of this maximum current will increase with increasing slick volume.

A 100-foot by 5-inch boom containing 7500 gallons of diesel fuel would experience "moderate" losses by entrainment in a 0.85-knot current. Assuming that the lost volume was continually replenished ahead of the boom, the volume lost would amount to 2700 gallons per hour.

D. Boom Geometry

Tests were conducted with various model configurations to investigate the effects of boom geometry and orientation on oil containment.

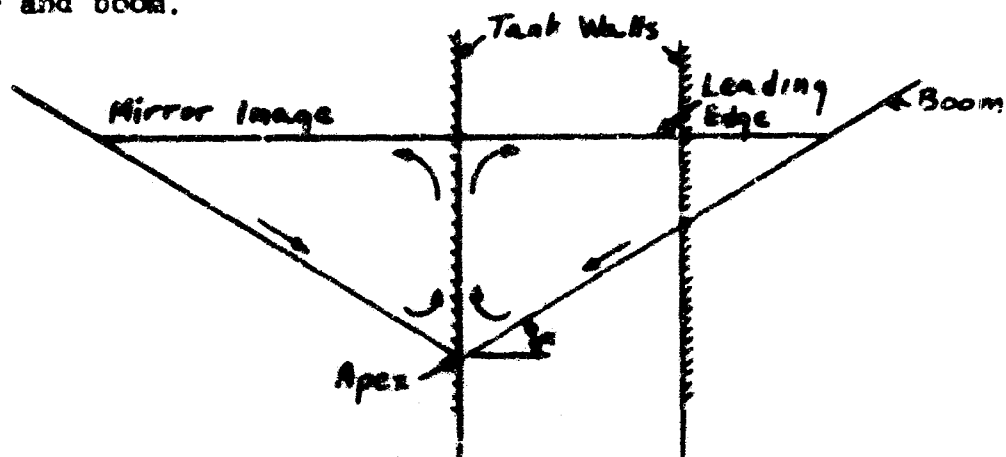
1. Boom Cross Section

Oil containment by the 90° wedge was essentially the same as by a flat plate. The only difference observed was that some entrained droplets are caught up in the eddy above the stagnation point of the flat plate, whereas any droplets reaching the wedge are carried under. This is a secondary effect. The inception of oil loss by entrainment and drainage and the volumes lost were not affected by this change in boom cross section.

c. Three-Dimensional Effects

Oil containment by angled flat plates ($\alpha = 30^\circ$ and 60°) was essentially the same as for the two-dimensional flat plate ($\alpha = 0^\circ$). The headwave remains two-dimensional, i.e., perpendicular to the direction of flow and uniform in cross section. Near boom effects caused by the intersection of the headwave and the boom are secondary.

A horizontal circulation was observed in the slick. Oil flow along the boom towards the apex is balanced by a net flow from the apex to the headwave and then out towards the intersection of the headwave and boom.



The volume of oil contained is, of course, not uniform along the angled boom and is greatest at the apex.

The observations noted above apply to the case where the slick is developed or contained ahead of the boom. It is possible that an angled boom could be used to deflect an "undeveloped" slick to the downstream end or apex of the boom for

collection. The slick would remain undeveloped only by withdrawing the deflected oil fast enough to prevent local thickening of the slick into the characteristic headwave. In this case it may be possible to use a boom without losing oil by entrainment or drainage in higher currents than for a developed slick. The present experiments do not support nor invalidate this supposition.

E. Effect of Waves on Oil Retention.

Experiments were conducted with combined currents and waves. Wave periods ranged from 0.5 to 1.0 seconds with wave heights up to 2.8 inches. As expected, waves generally degrade the containment performance of an oil boom.

1. Setup

The experiments show that substantial setup or thickening of the slick beyond the setup due to current is possible. No theory is available to predict this effect quantitatively. The model tests showed that setup due to waves was a complicated function of both wave height and frequency and is also affected by the boom's response to waves.

The photographs in Figure 29 show the effect of frequency on setup. Wave height and current are held constant. The inflated cylinder model is shown here with freedom in roll, heave and surge. The low frequency waves ($T = 1.0$ sec) are seen to have a negligible effect on slick length whereas higher frequency waves cause appreciable reduction of slick length. The headwave also becomes increasingly distorted by higher frequency waves. The oil thickness

in the slick is disturbed locally by the passing gravity waves with increased thickness corresponding to the wave crests and decreased thickness in the wave troughs.

This model is not sealed against the sides of the towing tank in order to allow free wave response. As a result, most of the oil seen behind the model in calm water was trapped behind the model from the start of the run while some is continually leaking past the sides during the course of the run. At the lowest frequency ($T = 1.00$ sec) oil is periodically entrained near the boom and passes under the skirt. At the highest frequency ($T = 0.50$ sec) oil has begun to drain freely under the skirt. At the middle frequency the loss is a combination of periodic entrainment with some drainage.

The single parameter which was found to have the most consistent influence on oil setup is the wave steepness ratio, the wave height divided by wave length H/λ . Figure 30 presents experimental data with the model shown in Figure 29 and Model 3 in Figure 20. The mean slick thickness in waves divided by the mean slick thickness in calm water, t_w/t_c , is plotted as a function of wave steepness. The mean thickness is defined as unit volume contained divided by the slick length. (Oil setup is shown as a function of wave height and period in Figure 31.) The steepness of large ocean waves may range from 0.04 to 0.18. Thus, we may expect that oil setup due to waves may increase the requirement for barrier depth to prevent drainage by a factor of 2.0 unless allowable current in waves is reduced by a factor of 1.4. It is possible that even steeper waves will be encountered in a wind driven chop.

Tests were also conducted with the model locked in heave, surge, and roll. High frequency waves with lengths less than 3 times the boom draft were completely reflected by the boom with the result that there was no setup due to these waves. Thus, waves in a wind driven drop whose lengths are less than 3 times the boom draft may not cause setup if the surge natural period of the barrier is large (about 3 times) compared with the wave periods.

2. Entrainment

It has been observed in our experiments that the orbital velocities at the wave crests tend to augment the current and cause the headwave to break up into droplets. Effective additions to the current velocity of from 20 to 70 percent of the orbital velocities were observed in tests by noting the current speeds at which droplets first formed in waves and in calm water. These observations apply only to cases where the gross qualities of the headwave were not appreciably altered by the waves, i.e., the wave steepness $H_w/\lambda < 0.04$. In steeper waves, the normal calm water headwave geometry can no longer be discerned at the leading edge of the slick. (In Figure 29 the values of wave steepness are 0.046, 0.040, and 0.023, corresponding to periods of 0.5, 0.75 and 1.00 second respectively.)

In addition, as steep waves enter the contained slick, they steepen further and break. This results in the formation of oil droplets at the interface which may be entrained under the boom.

Since these waves break near the leading edge of the slick, it may be expected that long slick lengths will reduce the loss of oil by entrainment. However, oil setup is increased in waves so that the only practical means of preventing entrainment losses in waves may be to reduce the current relative to the containment boom.

3. Boom Geometry and Resonance Effects

Losses can occur from the slick near the boom as a result of the relative motions between the boom and waves. These losses are a function of the boom's cross-section shape and heave, surge, and pitch freedom. The most critical condition appears to occur when a boom is restrained in surge but free in pitch. In this case large pitch motions were induced by the periodic relative surge velocities. Horizontal vortices were formed under the boom which entrained oil from the slick. When the models were restrained in the pitch direction by a towing bridle, the tendency to form horizontal vortices was greatly reduced. If compliance is provided in surge, the boom's relative motions were very small, and in this case there was very little tendency for near boom entrainment.

Near boom entrainment was a problem with the inflated cylinder model in high frequency waves where the boom heave response was out of phase with the waves. The large discontinuous increase in waterplane area near the waterline caused significant agitation of the slick. Comparative tests with the alternate designs, A-1 and A-2, showed them to have little agitation due to

out of phase heave motions. In all other respects, however, the alternative designs had comparable containment ability in waves when towing constraints, i.e., towline spring constant and bridle configuration, were similar.

Quantitative data on near boom entrainment are very difficult to obtain. In the case of the boom model A-2 with very little surge compliance, tests conducted with Zonyl A give some indication of the full scale relative velocities at which near boom entrainment will occur. These tests scaled to a 12" deep boom in 8" waves with a period of 1.5 seconds. Losses near the barrier started at scaled current speed of 1.5 ft/sec. This amounts to a maximum relative velocity at the bottom of the boom of about 3 ft/sec or an oscillatory velocity amplitude of about 1.5 ft/sec.

F. Multiple Boom Studies

Multiple boom configurations were briefly studied to find out if they might enhance containment ability over single booms. Two flat plate booms were used. Test variables were the draft of the forward boom and the longitudinal spacing between the two booms. Test results were mixed with some double boom configurations less successful at containment than a single boom.

To reduce oil entrainment losses we found that the spacing between two booms must be greater than the natural slick length with a single boom. When the spacing is equal to this slick length, the entrainment losses from turbulence behind the first

boom are greater than from the headwave with a single boom. By increasing the spacing by several times the forward boom's draft, the slick is effectively lengthened so that droplets entrained by the turbulence behind the first boom can rise back to the interface instead of flowing under the main collection boom.

The stretching effect of the forward boom can be seen by comparing the middle photograph in Figure 32 with the bottom photograph in Figure 23. With two booms the slick is about 80 percent longer (9 ft) than with a single boom (5 ft) at 1.40 fps current. The eddy region behind the forward boom is filled with oil. Behind this region the slick is quite thin and then gradually thickens toward the after boom. There is no headwave.

A more dramatic change in slick geometry is seen between the top and bottom photographs in Figure 32 at 1.60 fps current. The single boom has started to drain freely whereas with two booms the losses are due only to moderate entrainment.

The size of the eddy region behind the forward boom is roughly proportional to the boom draft. Experimental evidence in Reference 8 indicates the length of the eddy is about six times the boom draft. This length corresponds to the point at which the slick starts to become quite thin when the longitudinal boom spacing becomes large compared to the normal slick length. If the longitudinal spacing were too large with respect to the volume contained and depth of the forward boom, we expect that a headwave would be reformed ahead of the after boom and the slick in this region would behave similarly to the single boom case.

Under ideal conditions the double boom concept can increase the current speed for which oil can be contained. This increase is only on the order of ten percent or less and the additional complexity of such a system will probably not justify its use.

In summary, the slick lengthening made possible with a forward boom seems to be associated with the separated flow region behind this boom. Two booms are probably more beneficial for cases of small volumes than for large contained volumes which normally have long developed slicks. Entrainment of oil from the region behind the forward boom is not significantly different than normal headwave entrainment.

G. Absorbent - Ekoperl

Adding Ekoperl to an oil slick (four percent by weight) caused the slick length to increase up to 20 percent in currents near the speed for inception of entrainment loss. The increased length may be attributed mainly to the increased volume of oil plus absorbent. The oil soaked Ekoperl remains less dense than the oil and floats on top of the oil layer. Most of the Ekoperl is carried to the front of the slick by the circulation in the oil. There was a slight reduction in the oil loss by entrainment with the absorbent added. This may be attributed to the increased slick length. Entrainment of oil becomes very heavy when current is increased about 15 percent over the inception speed. However, the oil soaked Ekoperl remains contained while the unabsorbed oil is lost under the boom. The remaining layer of Ekoperl starts to draw under the boom at 60 percent higher current.

The addition of absorbents to oil slicks offer a possible means for containment under adverse conditions. Of course, their use may introduce other problems of subsequent disposal or reclamation. A critical point seems to be that all of the oil must be absorbed to effect a significant reduction in oil loss rate. Oil which is not absorbed is not affected and is free to become entrained as before. The current at which an oil soaked absorbent will be lost by entrainment or drainage is undoubtedly a complex function of the specific gravity of the resultant mixture and its several physical properties.

V. CONCLUSIONS

1. Slick geometry can be approximated using a simple two-dimensional math model with empirical coefficients. Errors may arise when extrapolating to large scale. However, large scale tests or field experience should provide suitable corrections to the theory.

2. Current velocity is the single most important parameter affecting oil containment. Entrainment losses increase quite rapidly with increasing current and can be severe in currents greater than approximately one knot. Excessive entrainment rates in calm water will probably cause successful oil retention to be limited to currents below a maximum value in the range of one to two knots. Waves cause increased entrainment rates and will further reduce the allowable current for successful operation. It is not yet known to what extent sea state alone will preclude containment.

3. Containment failure can occur both by drainage and/or entrainment of droplets under the boom. Boom draft needed to prevent drainage in calm water is readily calculated. Additional draft to prevent drainage in waves can only be grossly approximated. Increasing depth beyond that required for drainage is probably not efficient. The resulting load penalties would not be justified by the relatively minor improvement in entrainment loss rates.

4. Present theories may or may not afford reliable prediction of the rates of oil droplet formation. Small scale model tests have limited application in this regard due to the great difficulty in controlling the necessary scaling parameters.

5. Oil retention with booms can be enhanced by maintaining relatively long slick lengths to minimize entrainment losses. Slick length can be increased by deploying the boom in a deep U configuration and by minimizing current relative to the boom.

6. Double booms and absorbents have limited usefulness. Double booms are more complex and are helpful only for a small range of parameters. Two booms can be worse than a single boom in some conditions. Large volumes of absorbent material are required because all of the oil must be absorbed for the absorbent to be effective. Use of absorbents may be predicated on available collection and handling equipment.

7. Model test results have been valuable for empirical determination of coefficients to use with the theoretical expressions that have been developed. Some error is likely, however, when extrapolating model scale data to prototype scale. The important scaling parameters are Froude number, Weber number and Reynolds number. It is not possible to perform scale model tests with all these parameters satisfied simultaneously. Thus, complete simulation is only possible at full scale. However, some success has been obtained in scaling both Froude and Weber number. An approximate simulation over a limited scale ratio can be obtained by this technique.

8. The boom's cross section and dynamic response in waves can have some effect on losses caused by near boom entrainment from "washing machine action". Droplets are entrained into the flow just ahead of the boom when its motions are such that large relative velocities occur between the boom and surrounding fluids, e.g., when the boom has large out of phase pitch motions. The boom cross section should be smooth near the waterline so that heaving motions do not create large disturbances in the slick. Near boom entrainment can be reduced by increasing the boom's surge compliance. Pitch response should be restricted if large relative velocities at the bottom of the boom are induced by excessive pitch motions.

REFERENCES

1. "Design of a Light Weight Oil Containment System," Wilson Industries, Inc., Houston, Texas, June 1970.
2. Levich, V. G., "Physicochemical Hydrodynamics," Prentice-Hall, Inc., Englewood Cliffs, New Jersey, 1962.
3. Hinze, J. O., "Fundamental of the Hydrodynamics Mechanism of Splitting in Dispersion Processes," A.I.Ch.E. Journal, Vol. 1, No. 3, 1955.
4. Sleicher, C. A., "Maximum Stable Drop Size in Turbulent Flow," A.I.Ch.E. Journal, Vol. 8, No. 4.
5. Keulegan, G. H., "Interfacial Instability and Mixing in Stratified Flows," J. Res. NBS, Vol. 43, RP 2040, 1949.
6. Tulin, M. P. and Schwartz, J., "Hydrodynamic Aspects of Waste Discharge," AIAA Paper No. 70-755, AIAA 3rd Fluid and Plasma Dynamics Conference, July 1970.
7. Hoult, D. P., Pollack, V. G., and Reynolds, H. J., "Concept Development of a Prototype Lightweight Oil Containment System for Use on the High Seas," Johns-Manville Research Engineering Center, Part I Final Report, June 5, 1970.
8. Lindenmuth, W. T., "Experimental Study to Determine the Forces and Moments Acting on a Torpedo During the Launching Phase," (U), HYDRONAUTICS, Incorporated Technical Report 740-1, June 1967 (Confidential)
9. Keulegan, G. H., "The Motion of Saline Front in Still Water," NBS Report 5831, 1958.
10. Wicks, K., "Fluid Dynamics of Floating Oil Containment by Mechanical Barriers in the Presence of Water Currents," Joint Conf. on Prevention and Control of Oil Spills (API-FMPCA), New York, December 1969.
11. Wilz, E. A., "Evaluating Oil Spill Control Equipment and Techniques," Ocean Industry, Vol. 5, No. 7, July 1970.

HYDRONAUTICS, INCORPORATED

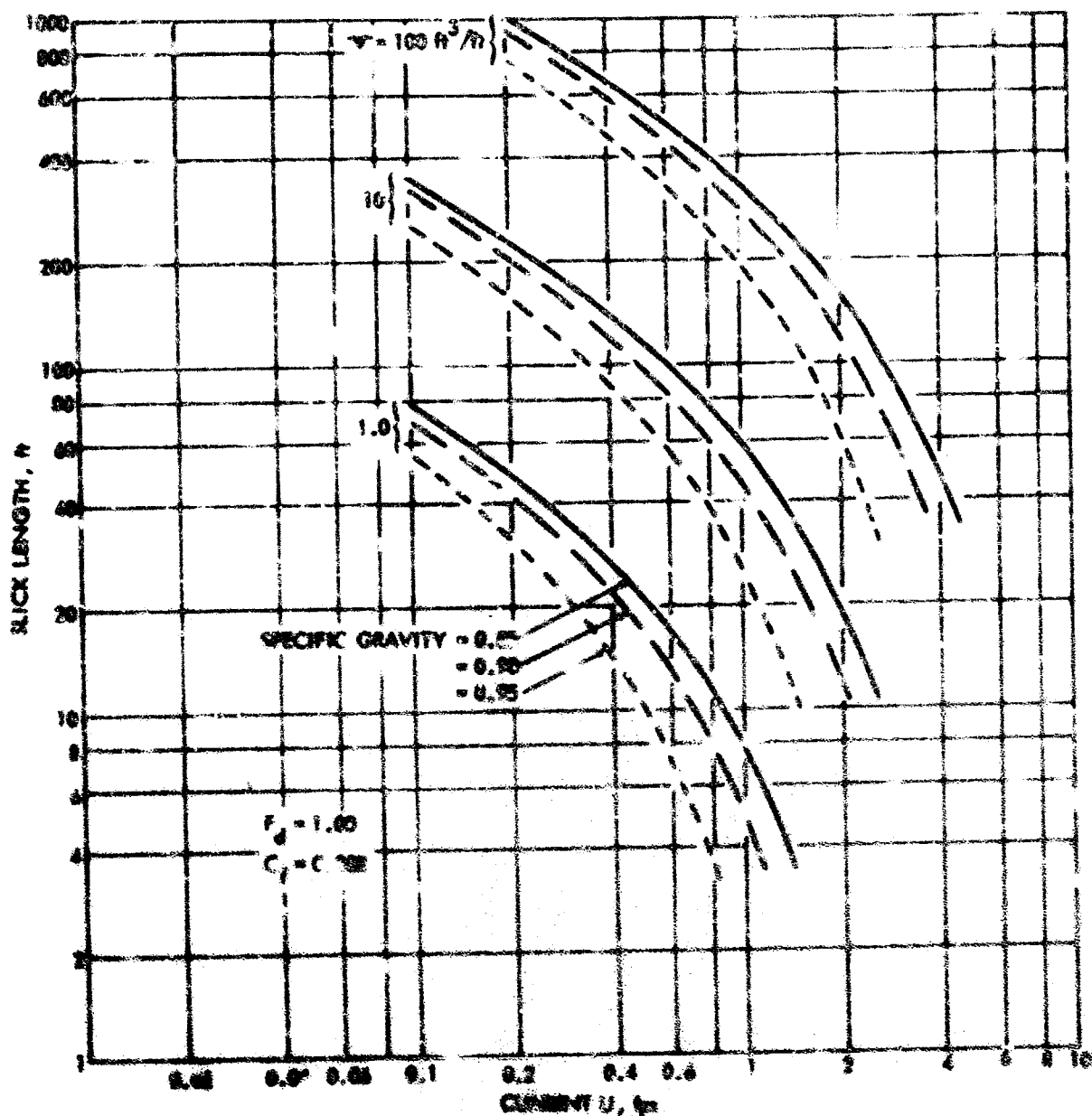


FIGURE 1 - TYPICAL CALCULATED SLICK LENGTH SHOWING VARIATION WITH CURRENT, CONTAINED VOLUME, AND SPECIFIC GRAVITY

HYDRONAUTICS, INCORPORATED

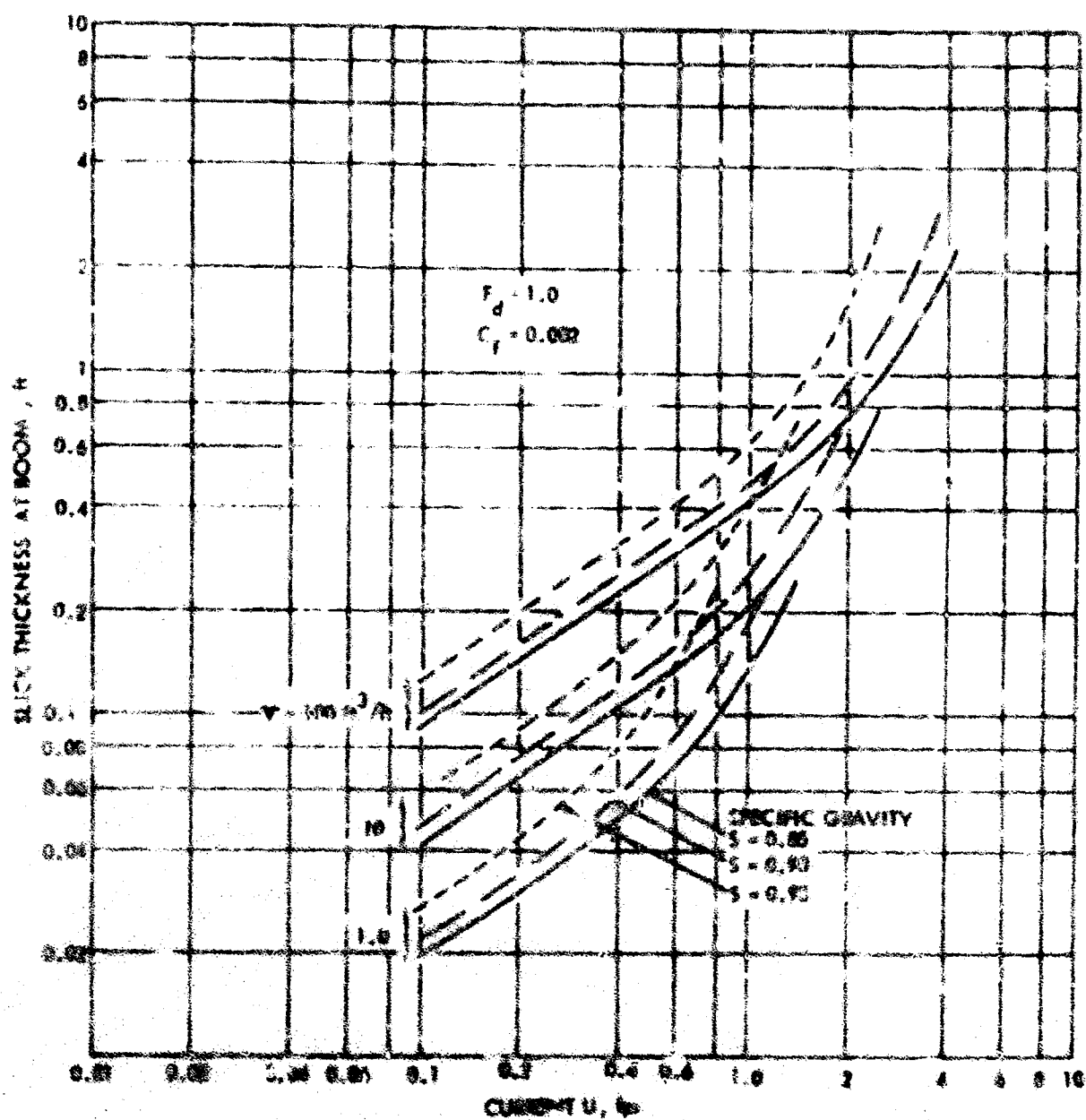


FIGURE 2 - TYPICAL CALCULATED OIL THICKNESS AT THE BOOM SHOWING VARIATION WITH
 OIL μ , OIL DENSITY, AND SPECIFIC GRAVITY

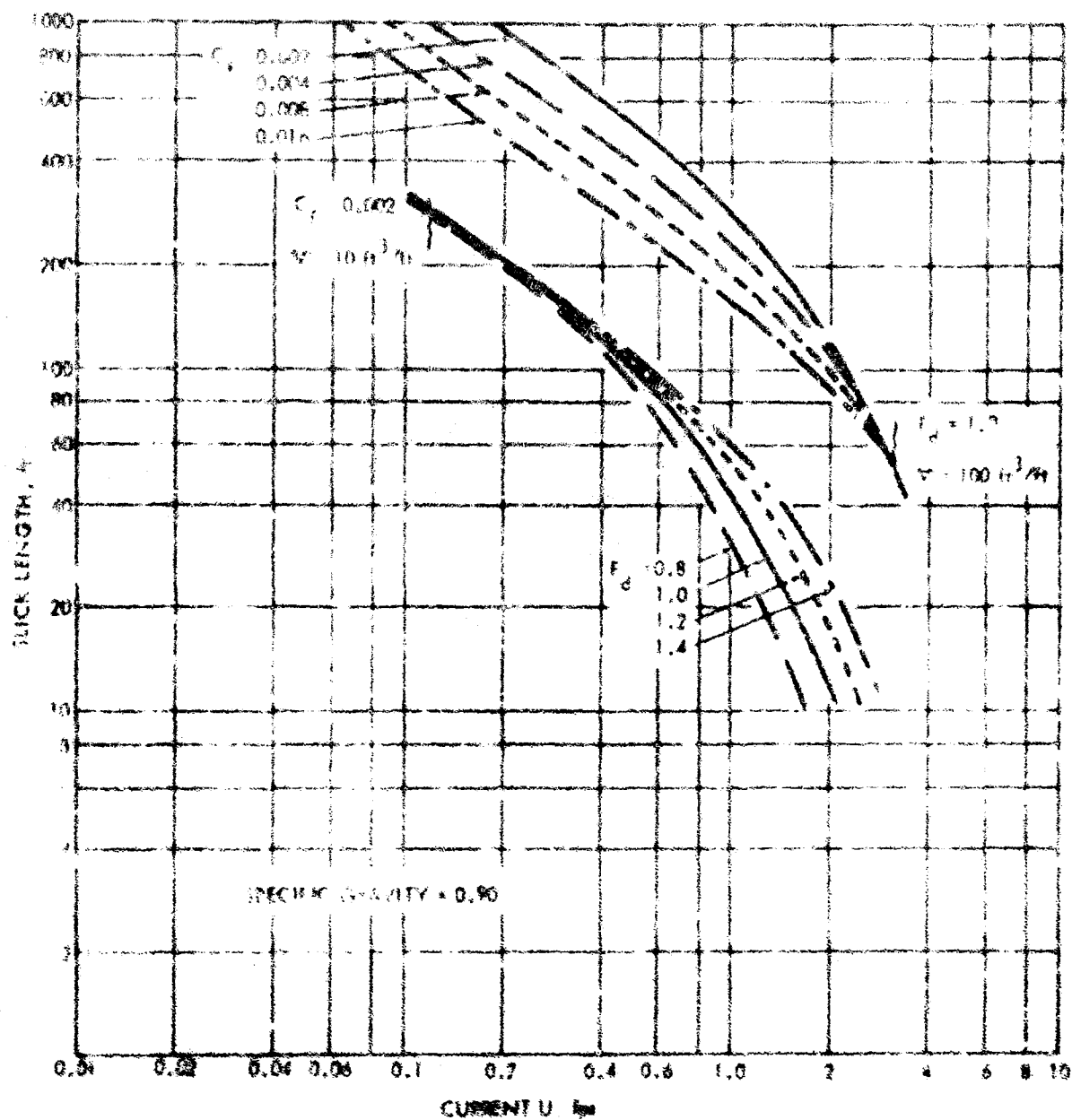


FIGURE 3 - TYPICAL CALCULATED SLICK LENGTH SHOWING VARIATION WITH CURRENT, HEADWAVE FROUDE NUMBER, AND INTERFACIAL FRICTION COEFFICIENT

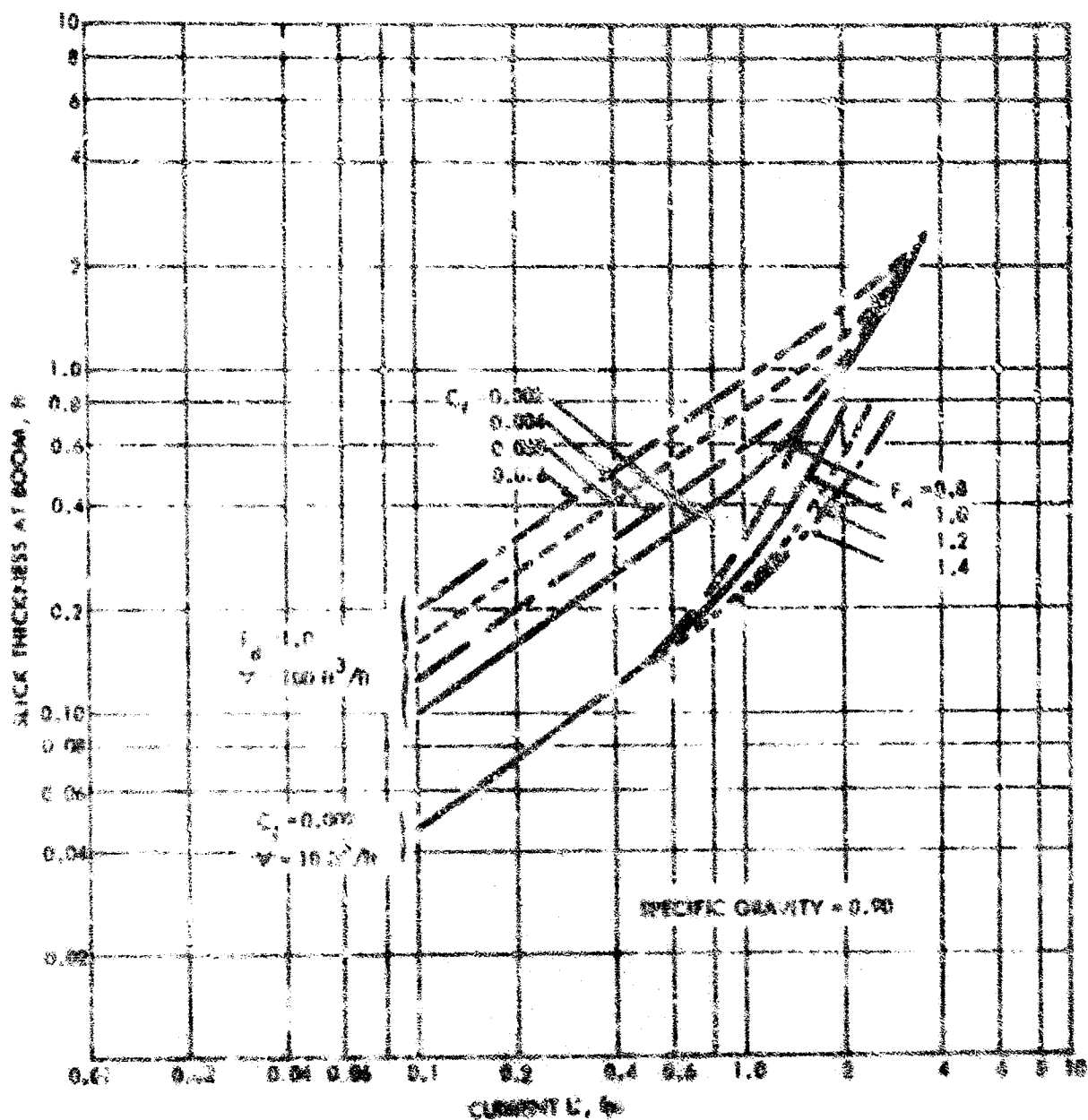


FIGURE 4 - TYPICAL CALCULATED OIL THICKNESSES AT THE BOOM SHOWING VARIATION WITH CURRENT, MAGNITUDE PICKUP NUMBER, AND INTERFACIAL FRICTION COEFFICIENT

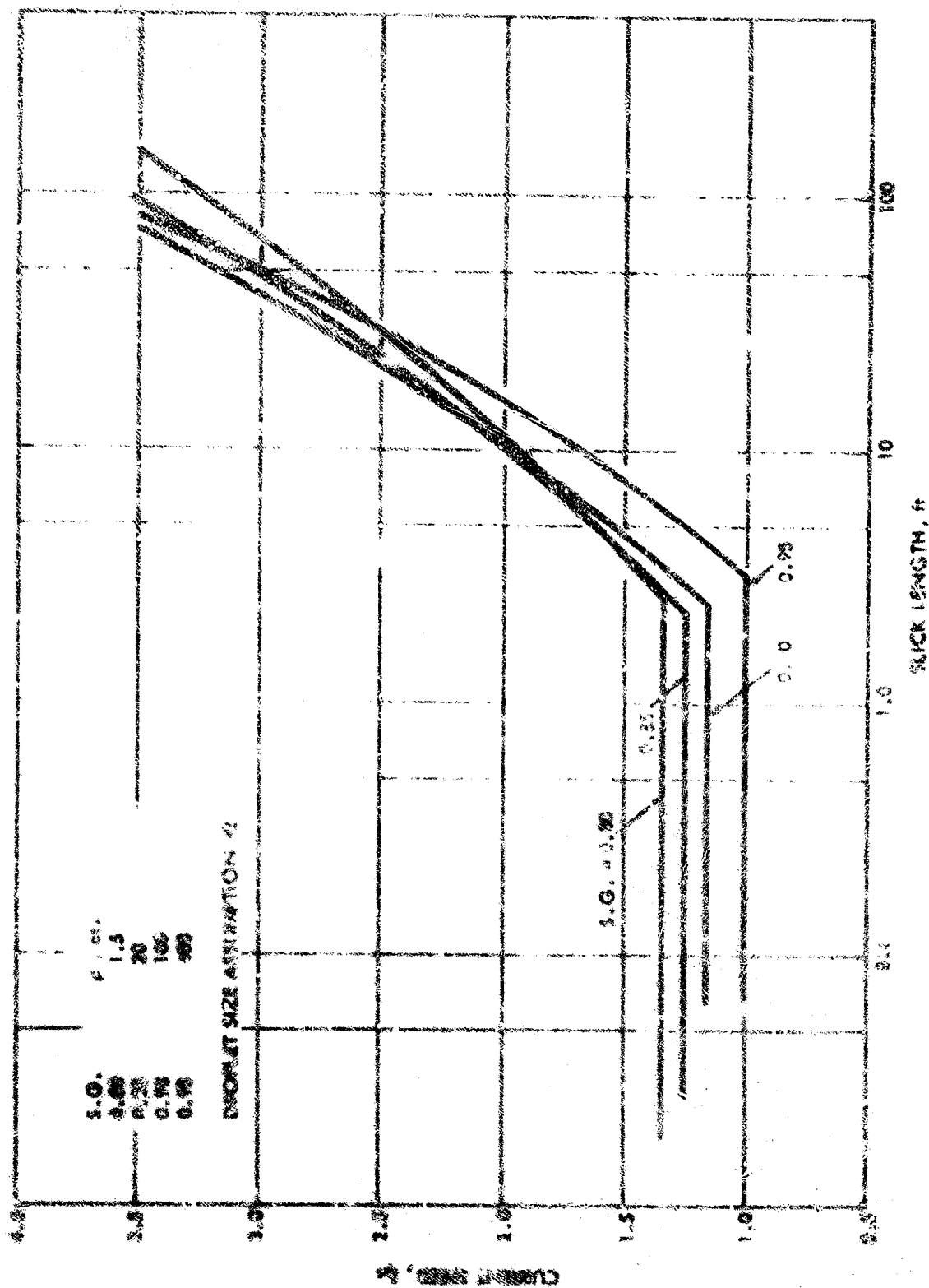


FIGURE 2 - CALCULATED MINIMUM SLICK LENGTH REQUIRED TO PREVENT ENTRAPMENT LOSS (OPTIMISTIC)

HYDRONAUTICS, INCORPORATED

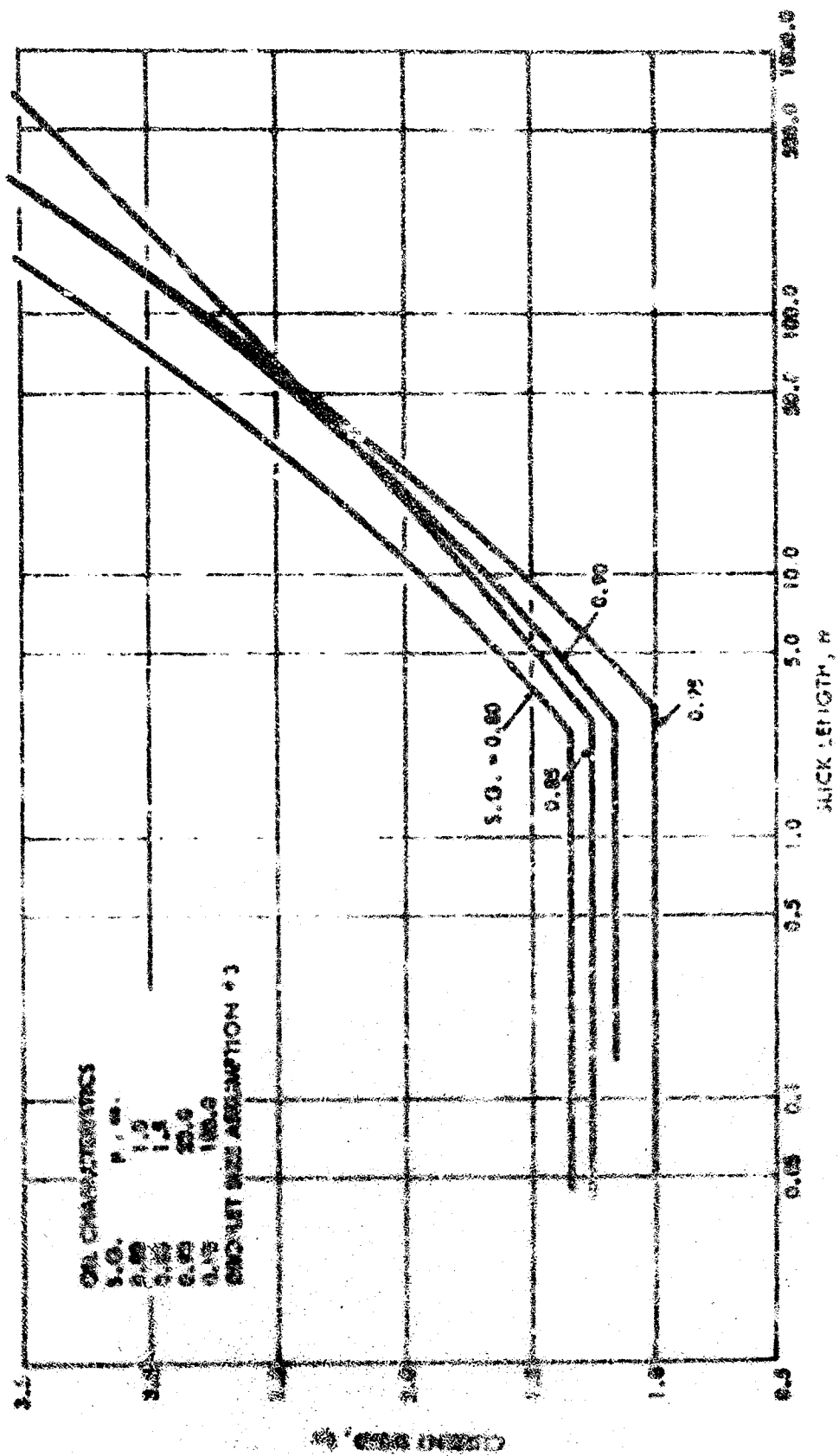
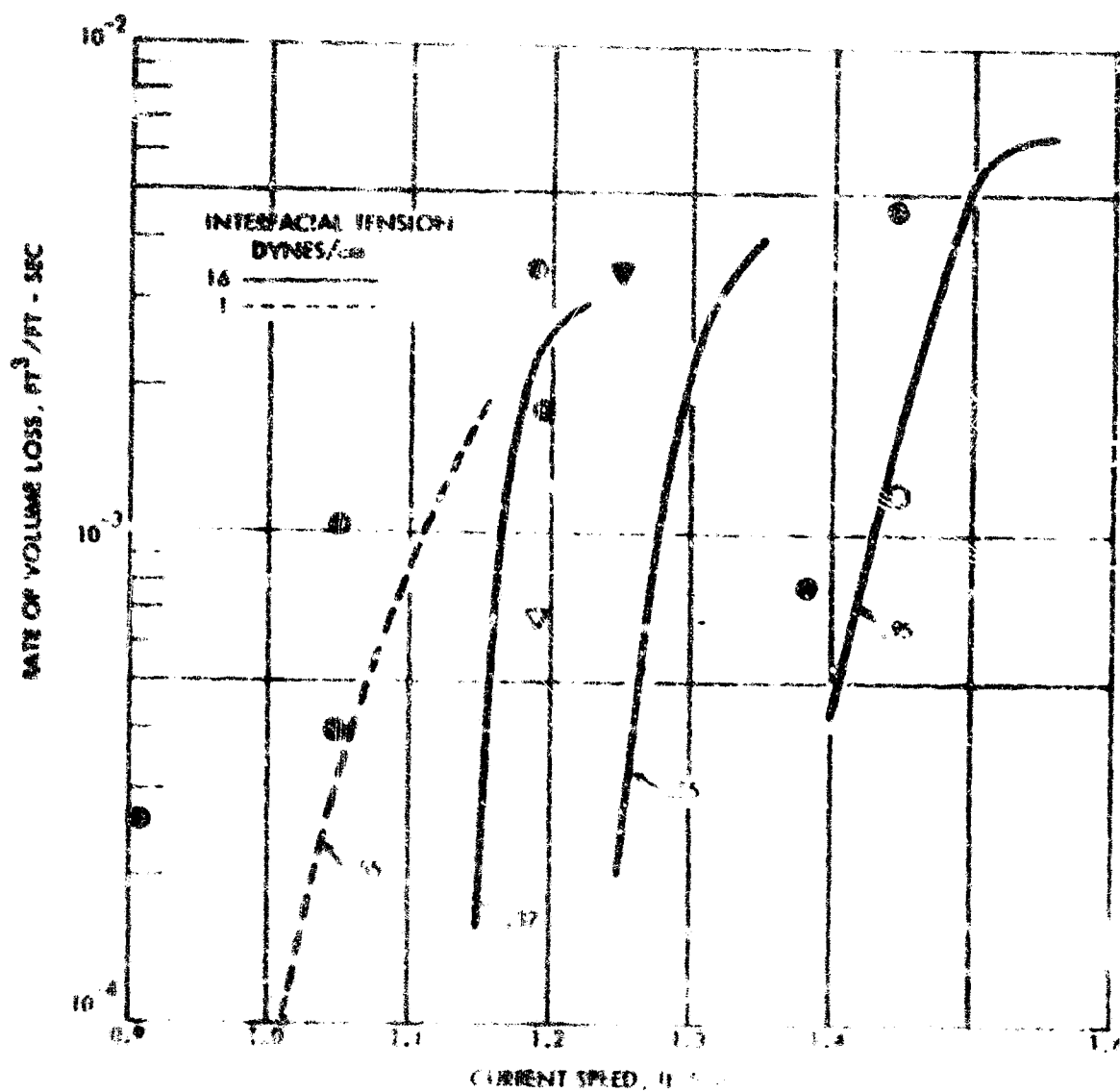


FIGURE 6 - CALCULATED MINIMUM SLICK LENGTH REQUIRED TO PREVENT ENTRAINMENT (LOSS PREVENTIVE)

HYDRONAUTICS, INCORPORATED



| | SYMBOL | SPECIFIC VOLUME, CONTAINED ft^3/ft | WATER LEVEL, IN. |
|----------|--------|---|------------------|
| MEASURED | ▽ | 0.37 | 5 |
| | ● | 0.55 | 4 |
| | ○ | 0.55 | 5 |
| | ⊙ | 0.95 | 5 |

FIGURE 7 - COMPARISON OF MEASURED AND CALCULATED ENTRAINMENT LOSS RATES

HYDRONAUTICS, INCORPORATED

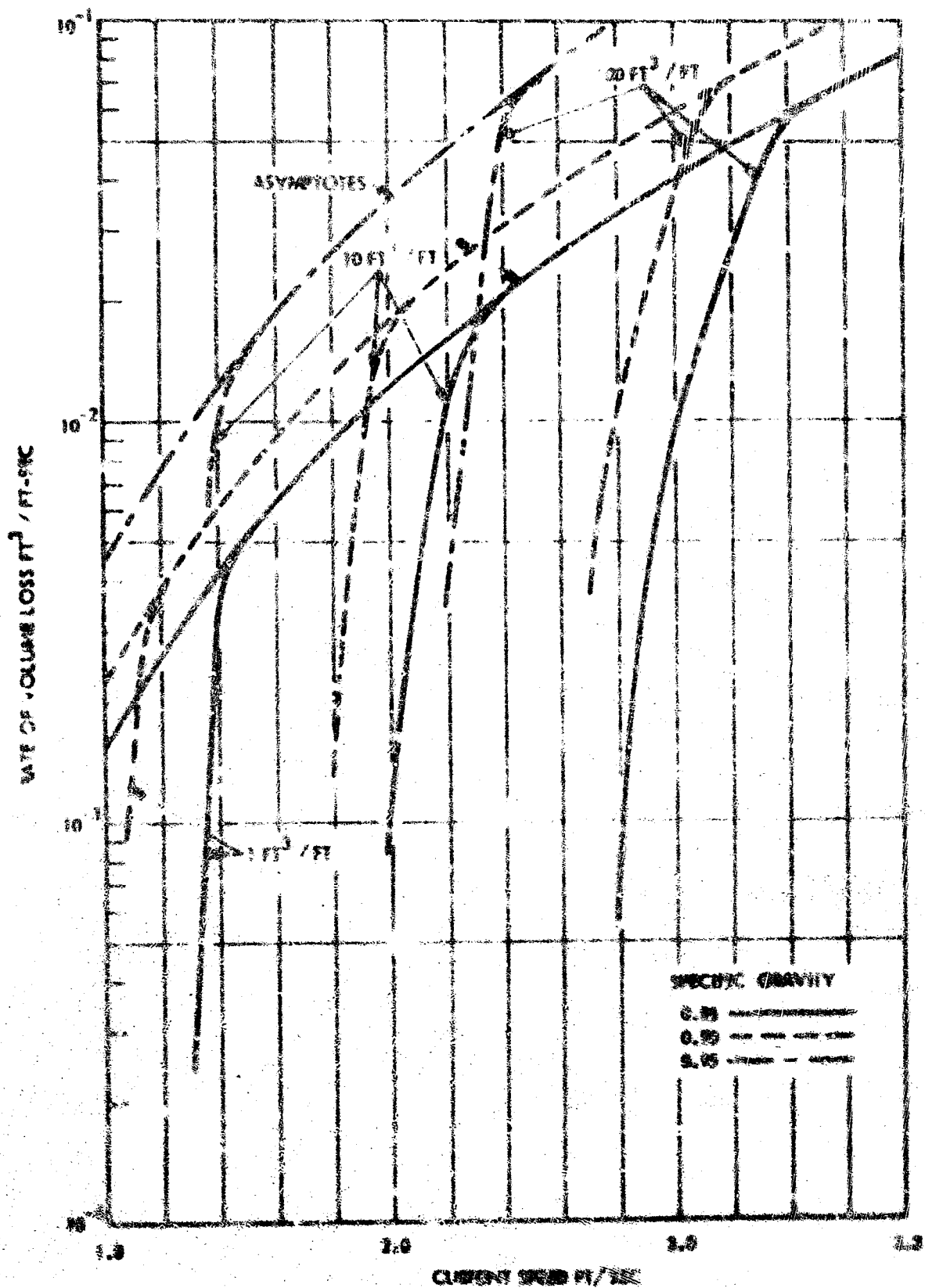


FIGURE 2 - UNWEIGHTED LOSS RATE AS A FUNCTION OF CURRENT SPEED, CONTAINER VOLUME AND SPECIFIC GRAVITY

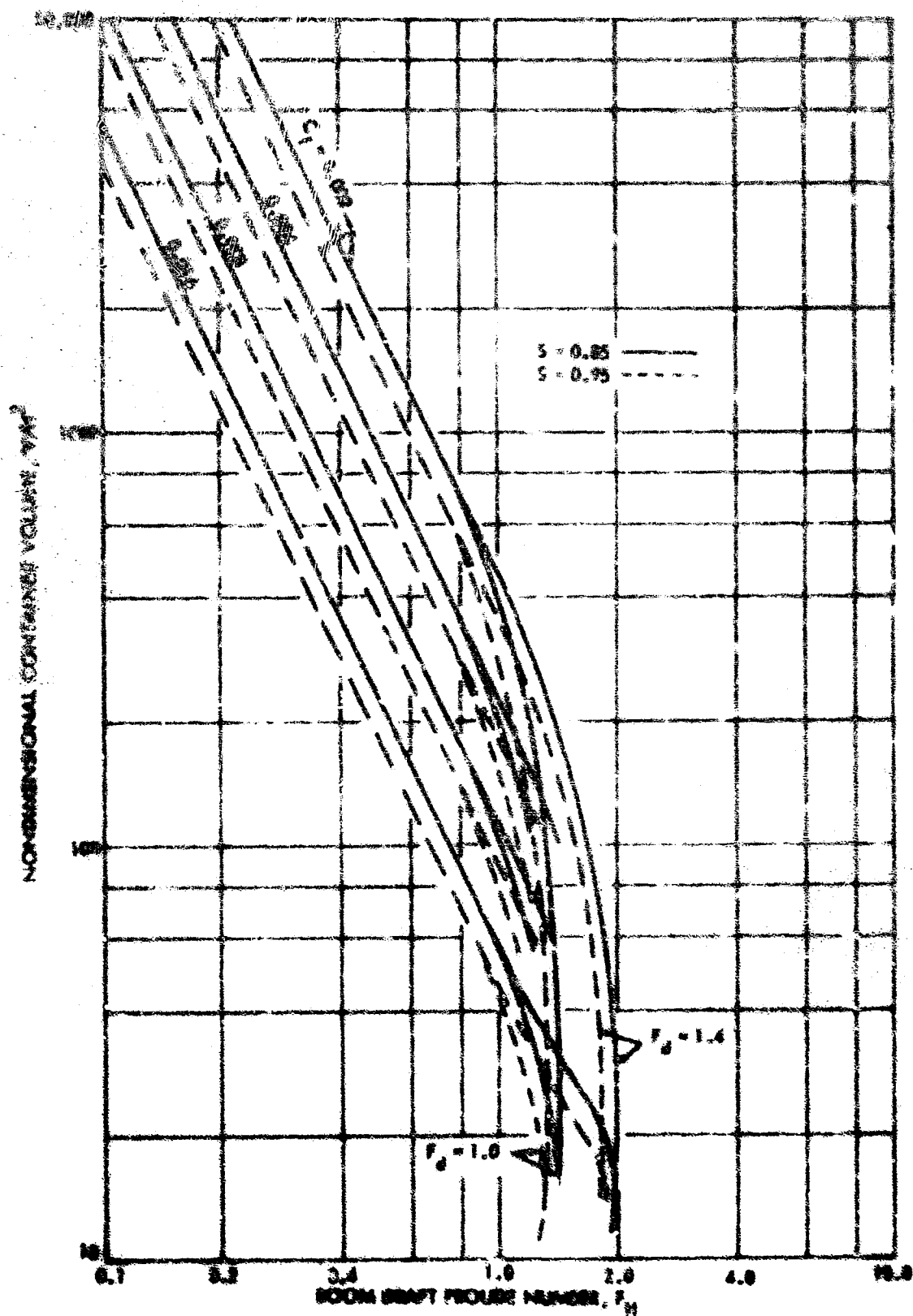


FIGURE 9 - MAXIMUM THEORETICAL VOLUME OF OIL CONTAINED IN CALM WATER

HYDRONAUTICS, INCORPORATED

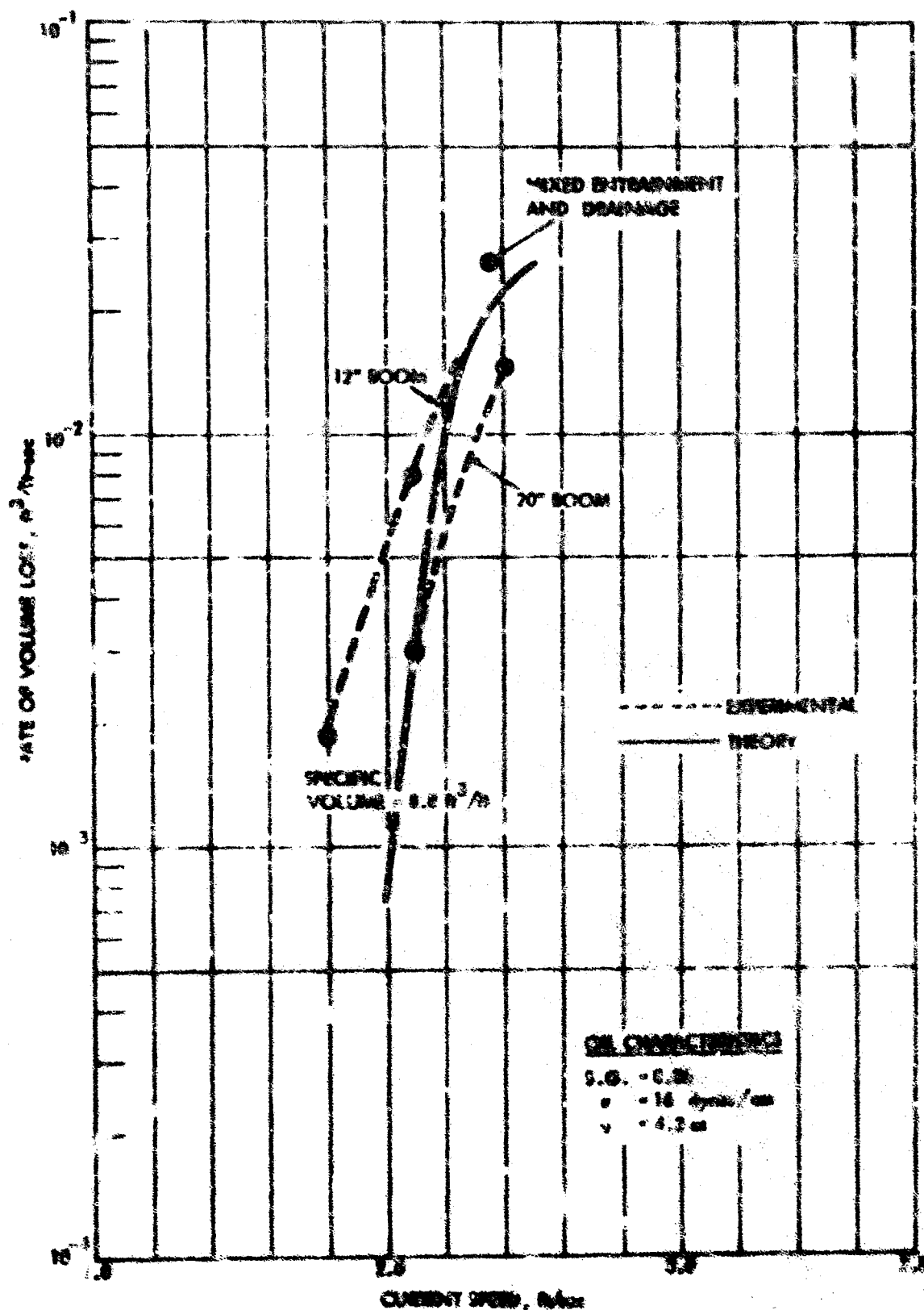


FIGURE 19 - EXPANSION OF TYPICAL SCALE MODEL DATA FOR OIL LOSS RATE

HYDRONAUTICS, INCORPORATED

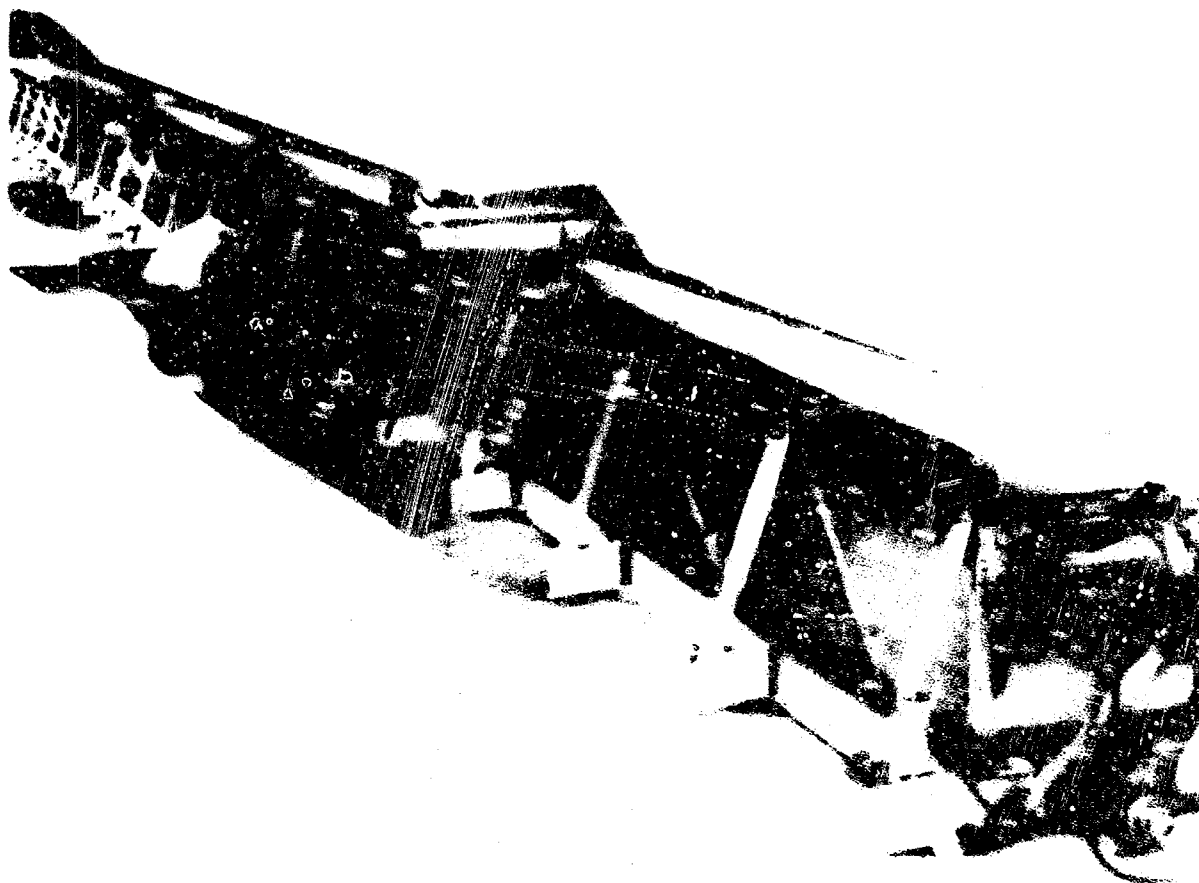


FIGURE 11 - PW OF 80 FT TOWING TANK

HYDRONAUTICS, INCORPORATED



FIGURE 12 - DETAILS OF THE HINGED PLATED WAVEMAKER

HYDRONAUTICS, INCORPORATED

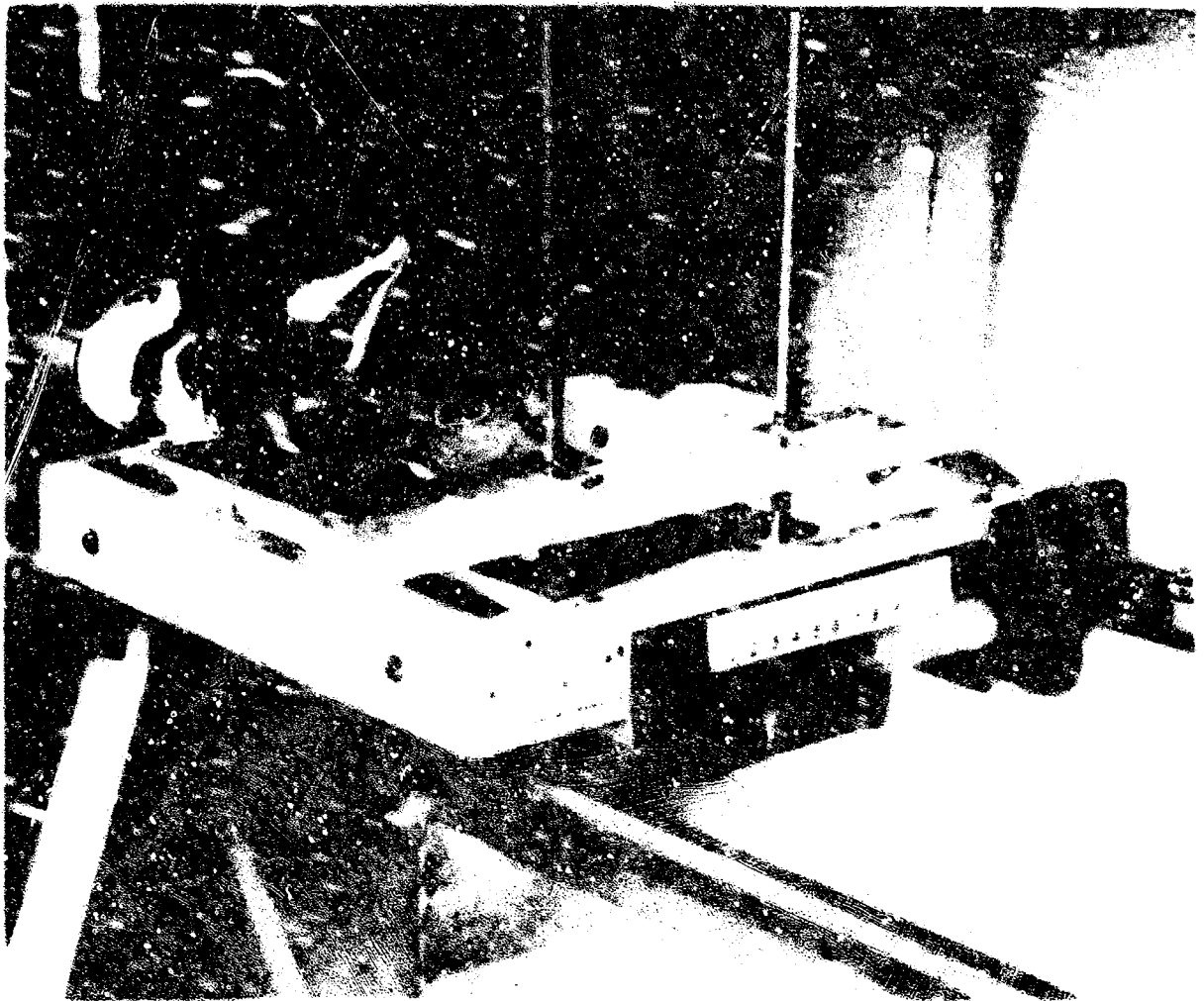


FIGURE 13 - VIEW OF THE TOWING CARRIAGE (SHOWN WITH FLAT
PLATE BOOM MODEL)

HYDRONAUTICS, INCORPORATED



FIGURE 14 - CARRIAGE DRIVE SYSTEM

HYDRONAUTICS, INCORPORATED

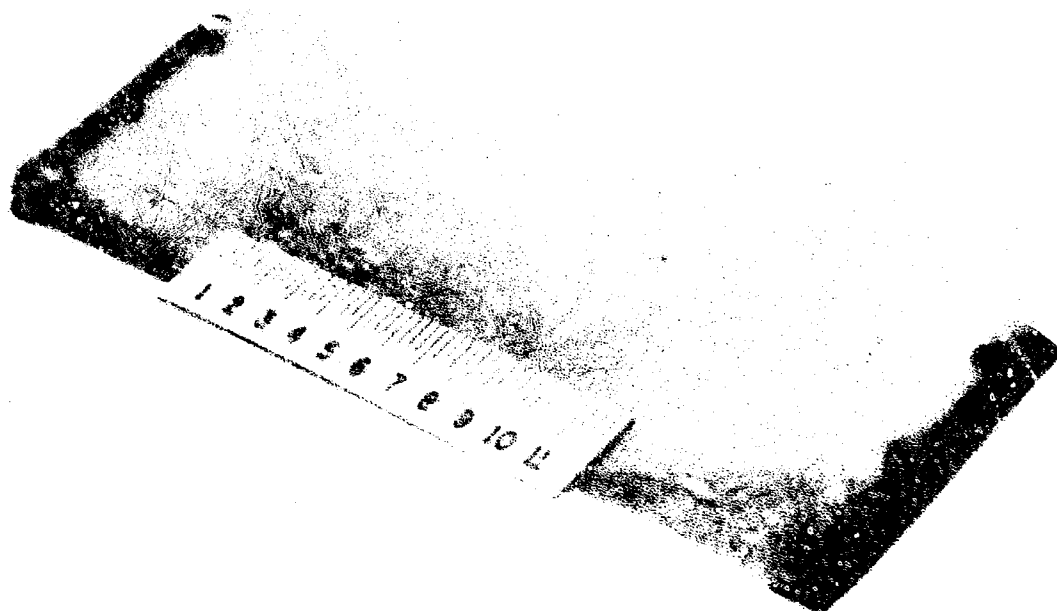


FIGURE 15 - FLAT PLATE MODEL

HYDRONAUTICS, INCORPORATED



FIGURE 16 - ANGLED BOOM MODEL, $\alpha = 30^\circ$

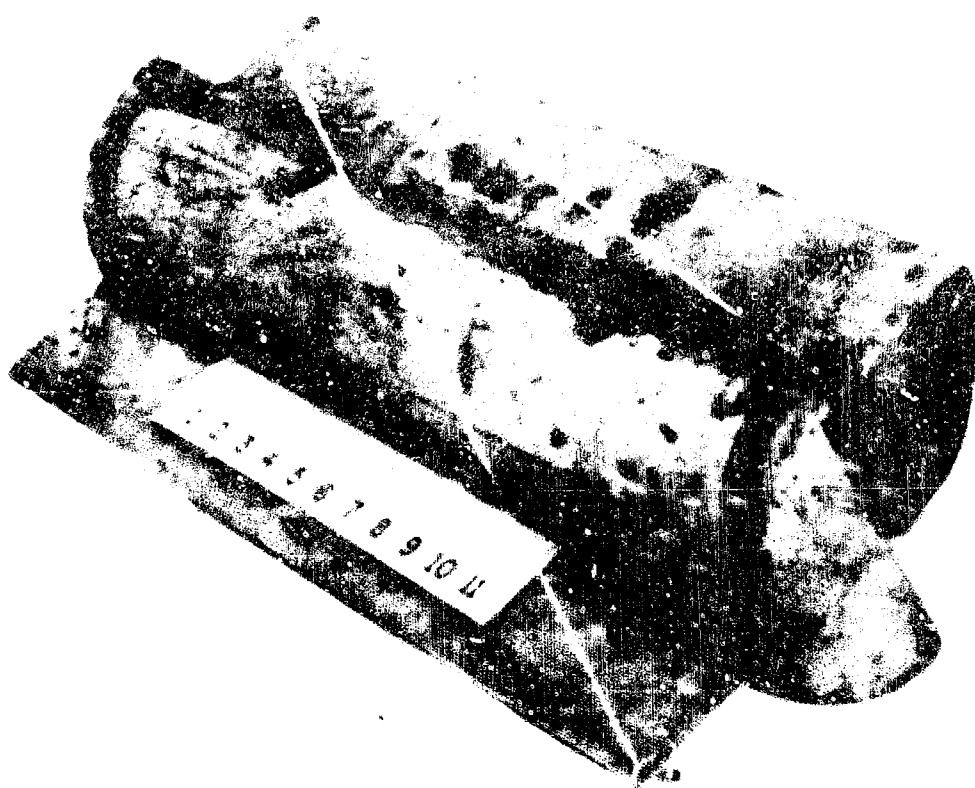
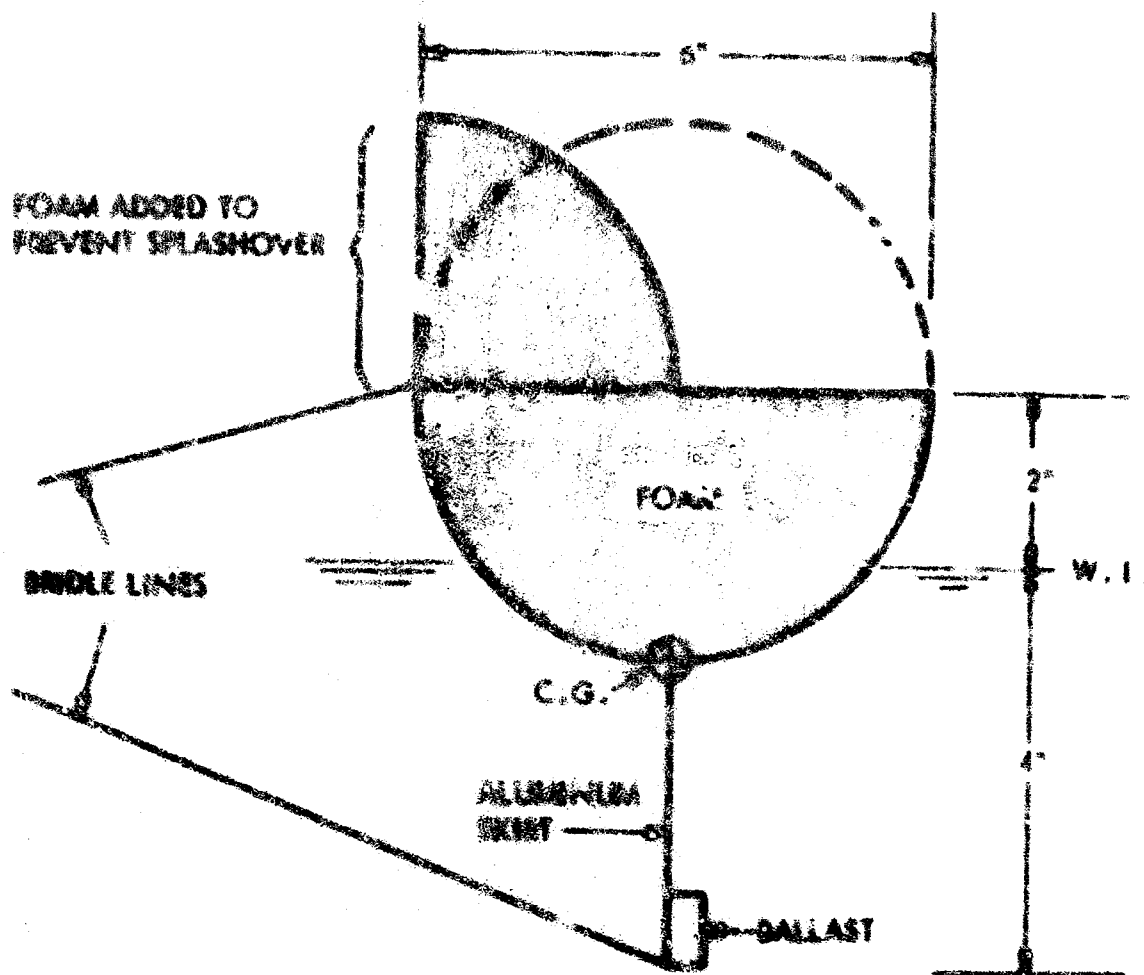


FIGURE 17 - INFLATED CYLINDER DYNAMIC MODEL

HYDRONAUTICS, INCORPORATED



MODEL WEIGHT = 3.61 LB

FIGURE 10 - DETAILS OF INFLATED CYLINDER DYNAMIC MODEL

HYDRONAUTICS, INCORPORATED

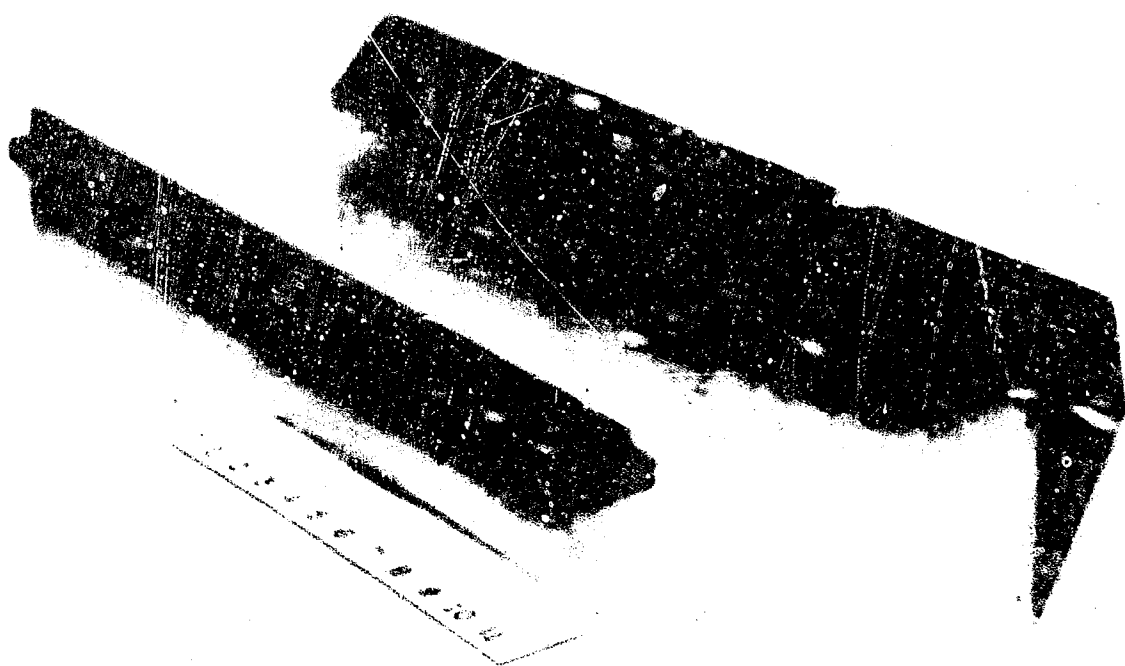
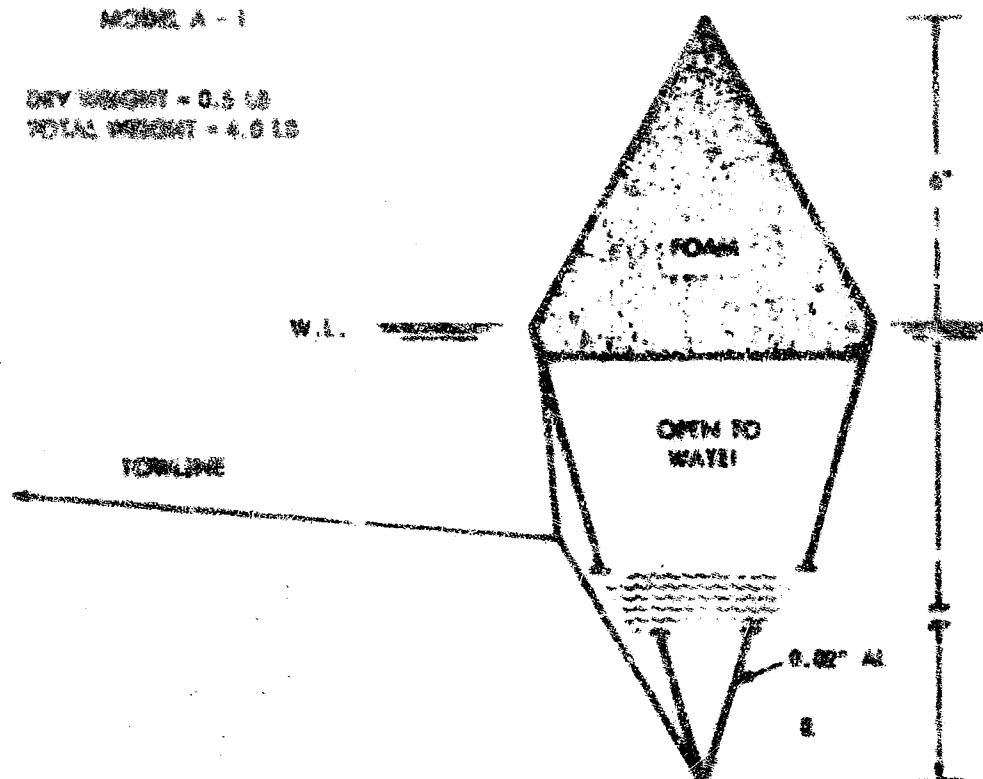


FIGURE 19 - TWO ALTERNATE DYNAMIC MODELS

HYDRAULICS, INCORPORATED

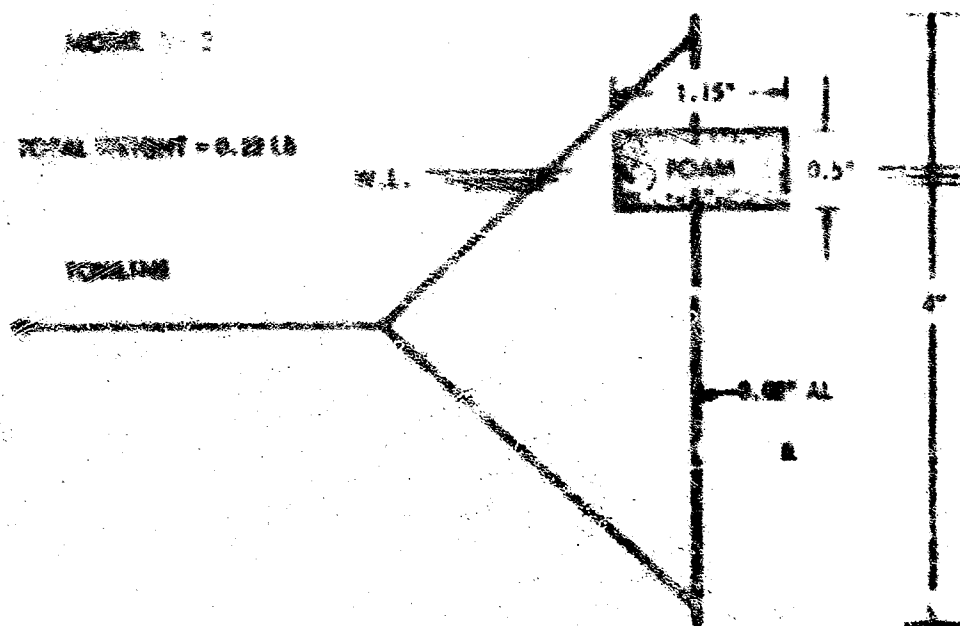
MODEL A - 1

DRY WEIGHT = 0.5 LB
TOTAL WEIGHT = 4.0 LB



MODEL A - 2

TOTAL WEIGHT = 0.22 LB



MODEL A-2 - DETAILS OF ALUMINUM MODEL

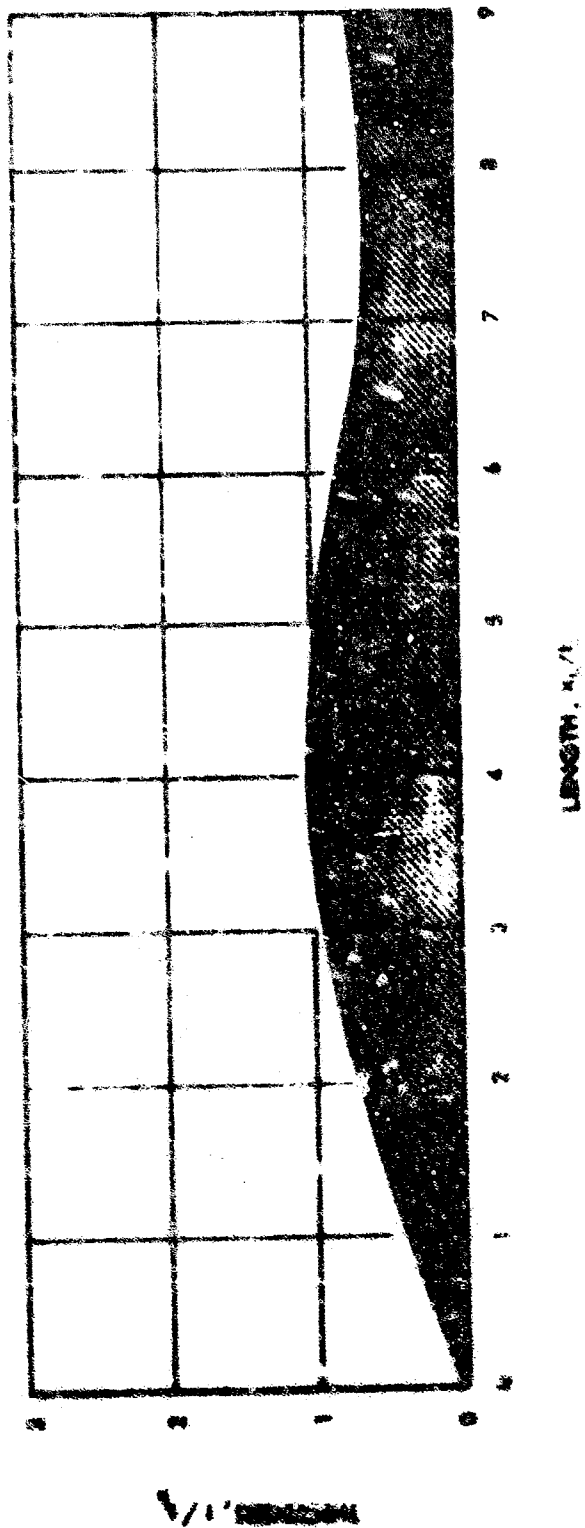


FIGURE 21 - MEASURED GEOMETRY

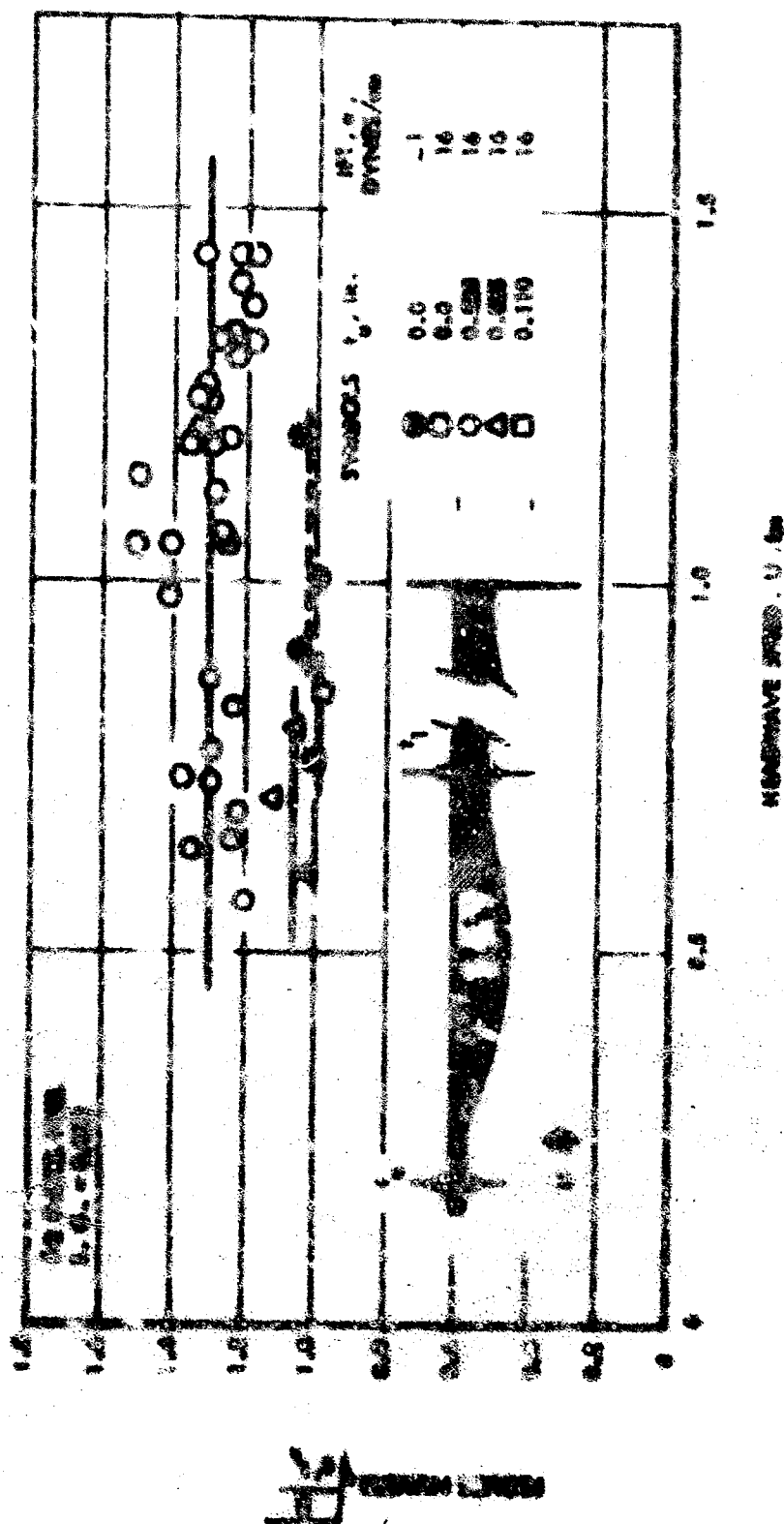
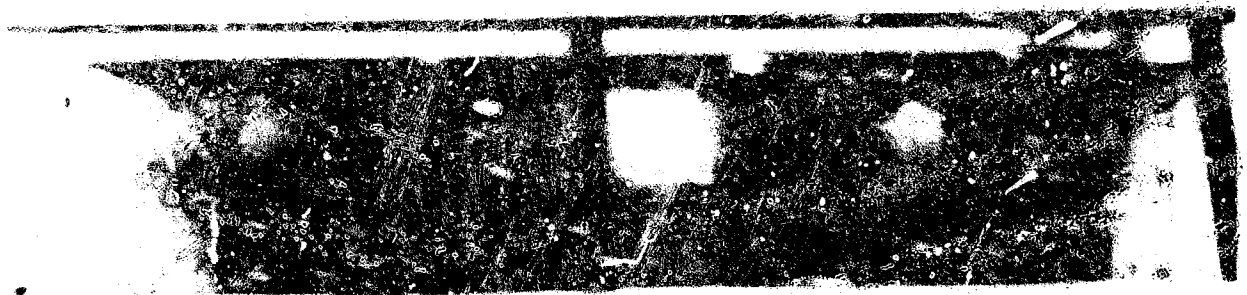


FIGURE 10 - CHARACTERISTIC WAVE HEIGHTS OF THE WAVE

HYDRONAUTICS, INCORPORATED



VELOCITY = 1.20 fps



VELOCITY = 1.30 fps



VELOCITY = 1.40 fps

FIGURE 25 - OIL SLICK GEOMETRY. #2 DIESEL FUEL. FIXED VOLUME = $1.0 \text{ ft}^3/\text{ft}$
BOOM DEPTH = 5 in.

HYDRAUTICS, INCORPORATED

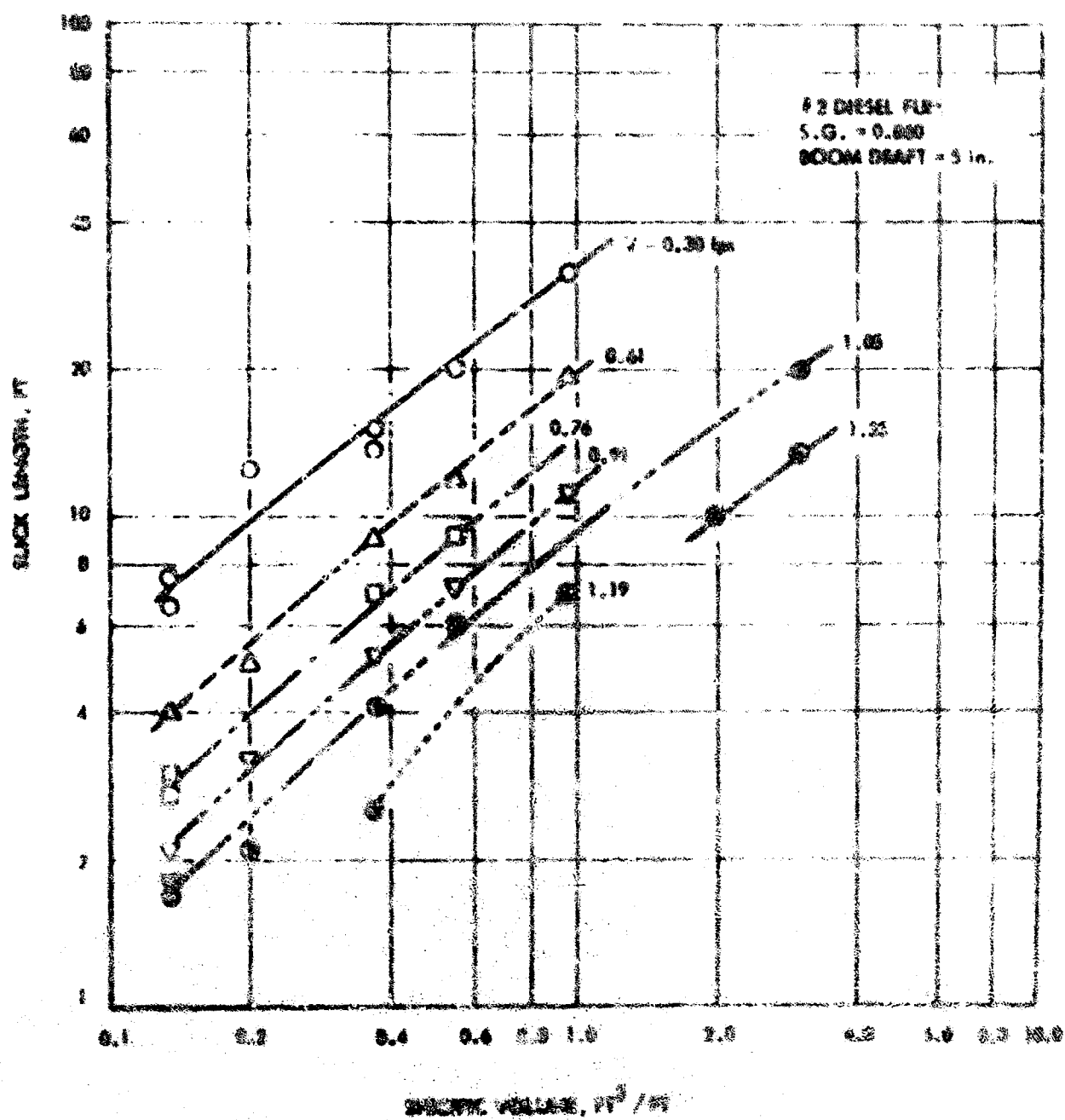


FIGURE 54 - DATA OBTAINED - DRAFT AND SLACK LENGTH AS A FUNCTION OF SPECIFIC VOLUME

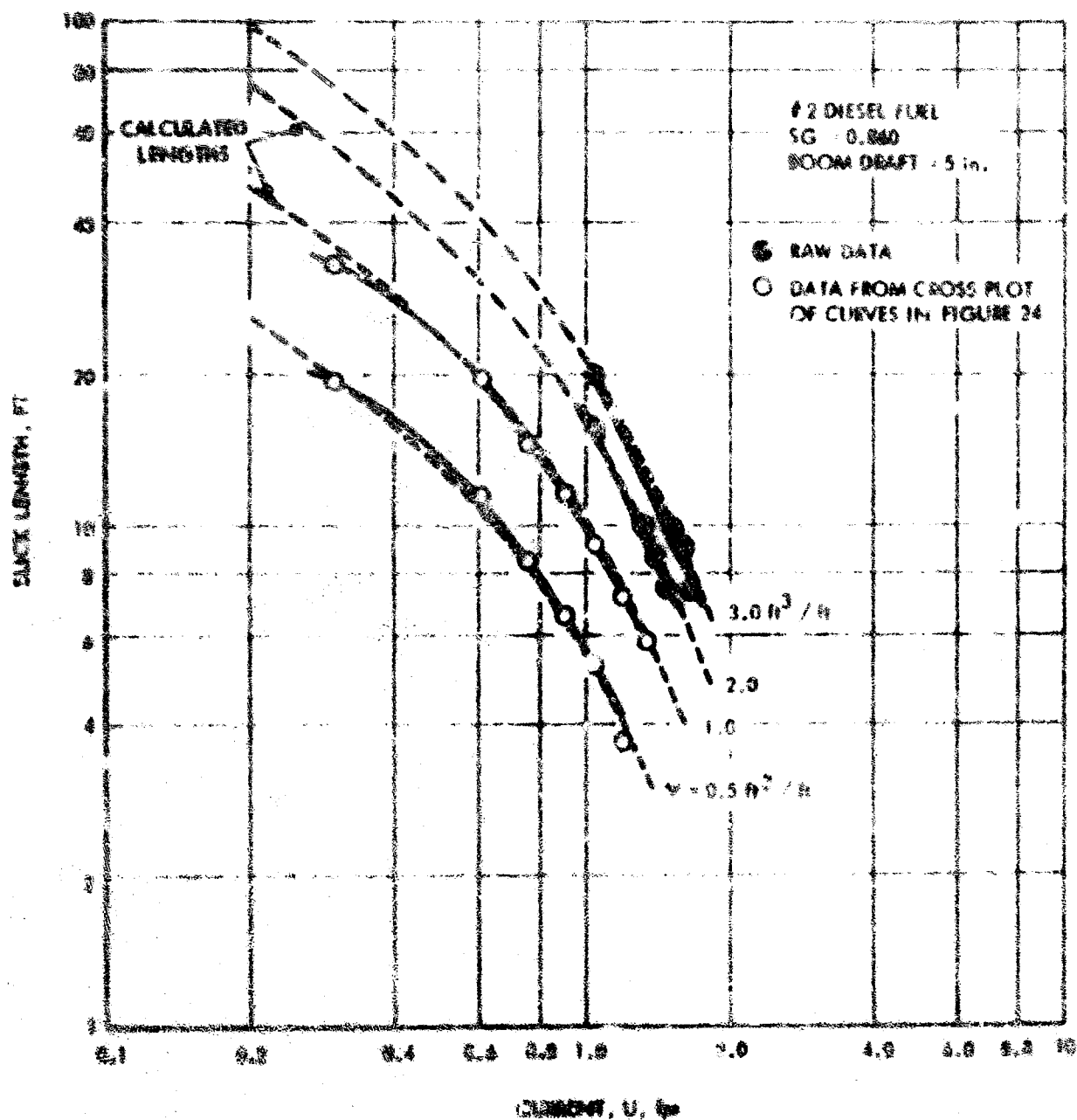


FIGURE 25 - DIESEL FUEL SLICK LENGTH AS A FUNCTION OF CURRENT VELOCITY
 (SHOWING COMPARISON WITH CALCULATED VALUES)

HYDRONAUTICS, INCORPORATED

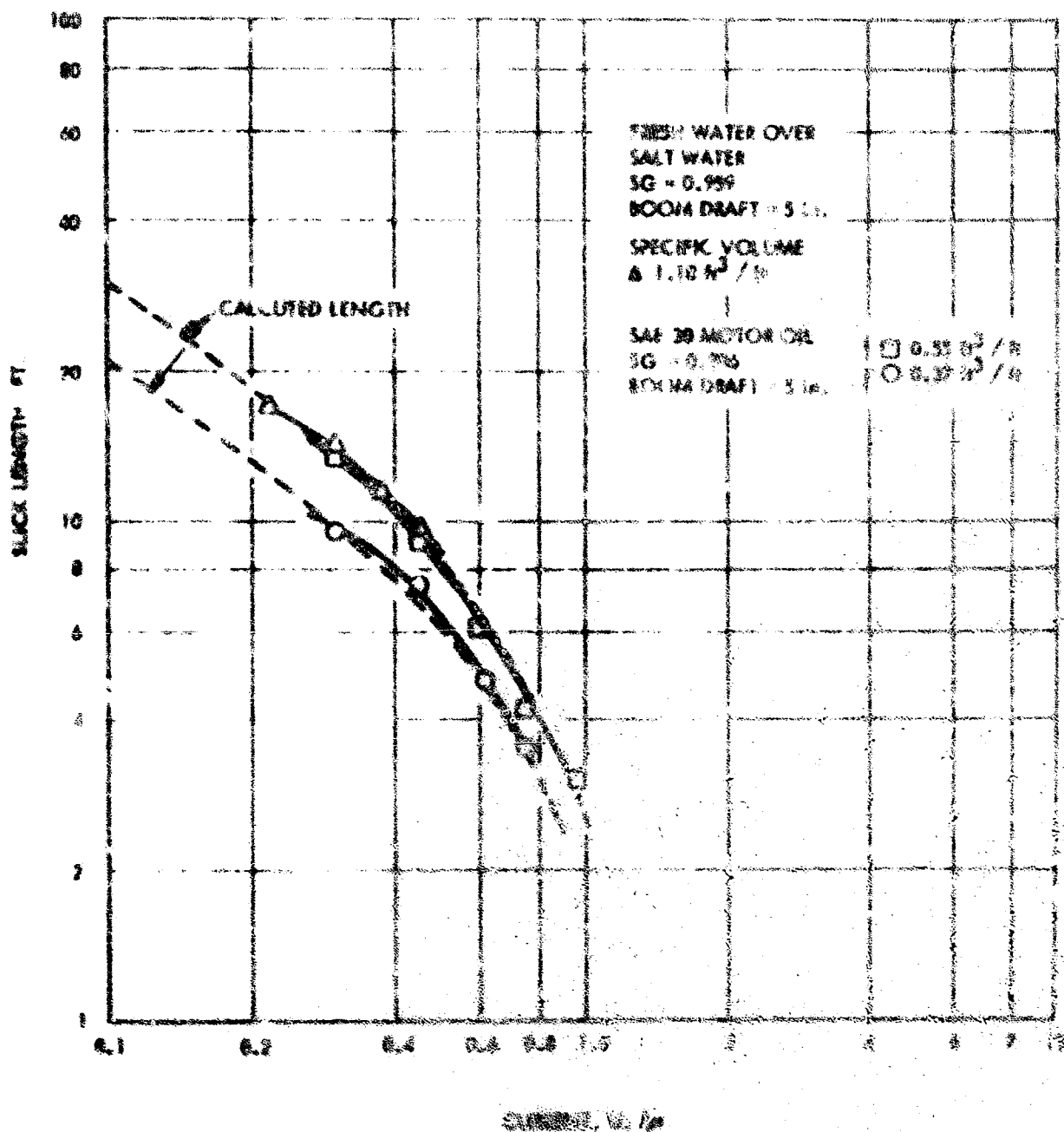


FIGURE 16 - SLICK LENGTH FOR MOTOR OIL AND FRESH WATER OVER SALT WATER

| SYMBOL | SPECIFIC VOLUME "CONTAINED" F^2/RT | FLAT PLATE BOOM DEPTH, IN. |
|--------|---|-------------------------------|
| ○ | 0.13 | 3 |
| □ | 0.20 | 3 |
| ▽ | 0.37 | 2 |
| △ | 0.37 | 5 |
| ● | 0.55 | 3 |
| ⊙ | 0.55 | 5 |
| ○ | 0.95 | 5 |

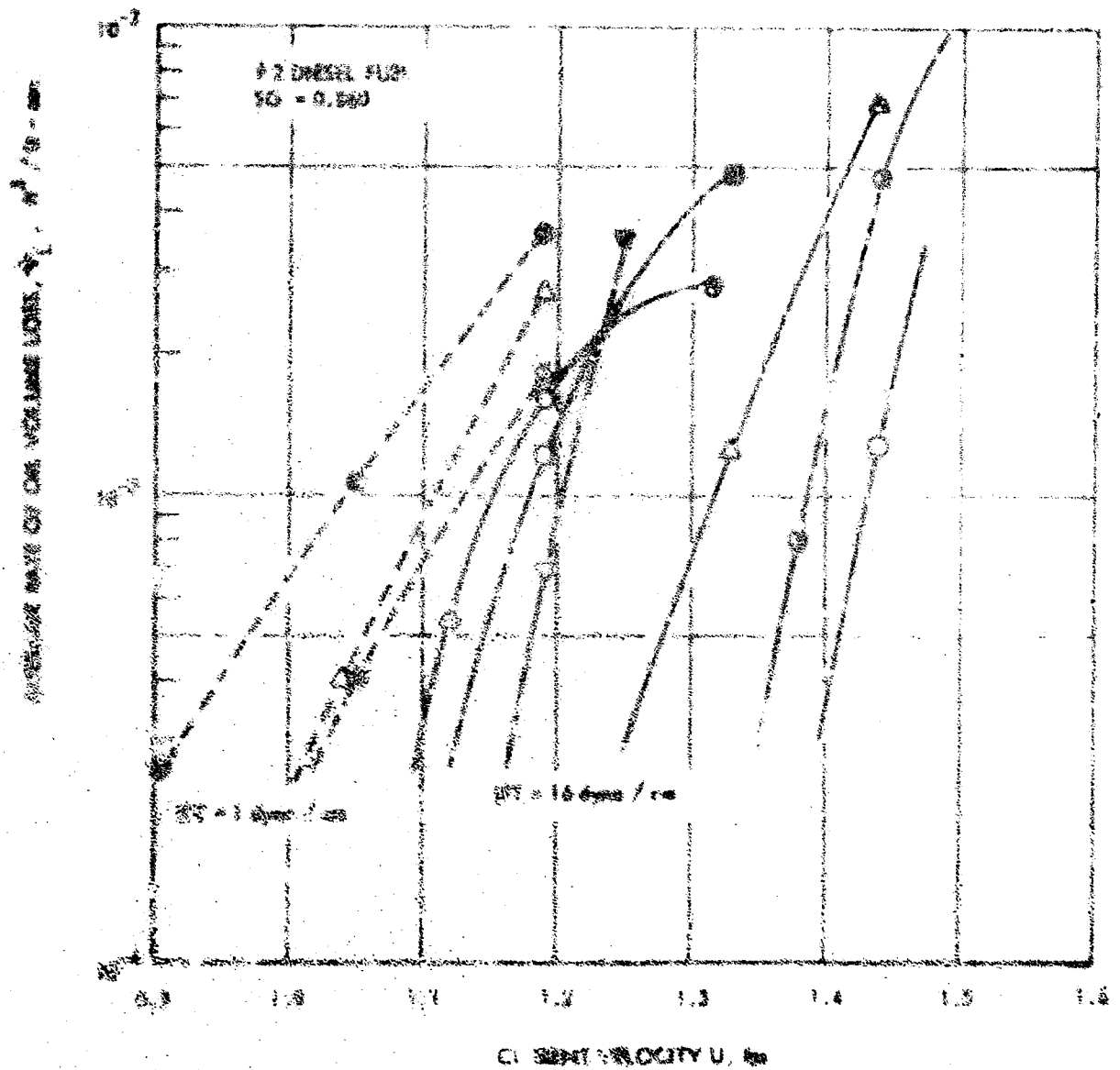


FIGURE 27 - DIESEL FUEL ENTRAINMENT LOSS RATES

HYDRONAUTICS, INCORPORATED

| SYMBOL | SPECIFIC VOLUME FT ³ / FT | INTERFACIAL TENSION DYNE / CM |
|--------|--|-------------------------------------|
| ○ | 0.37 | 18.8 |
| □ | 0.55 | 16.8 |
| △ | 0.55 | 12.8 |

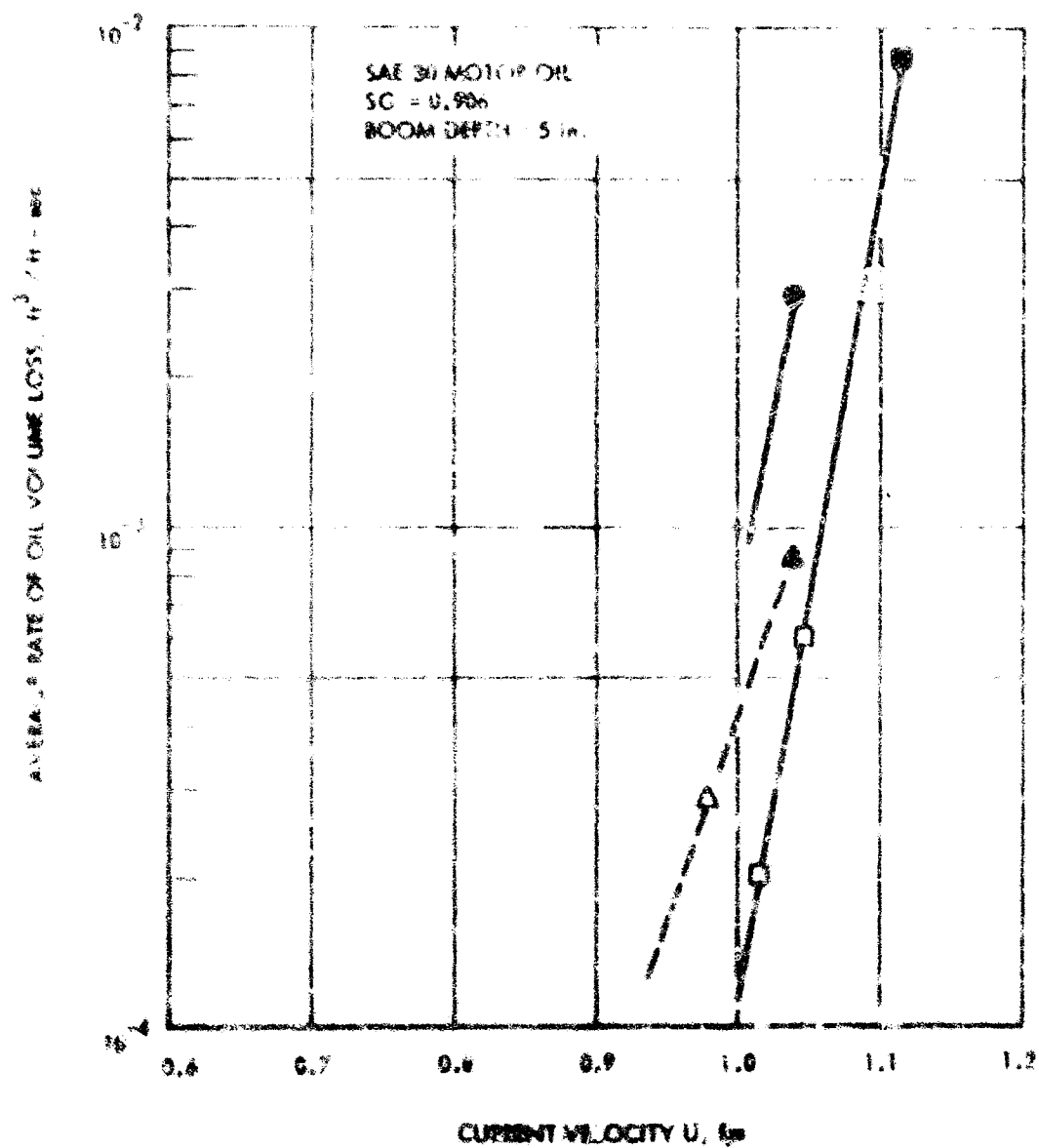


FIGURE 29 - THIRTY WEIGHT MOTOR OIL LOSS RATES

HYDRONAUTICS, INCORPORATED



$T = 0.5 \text{ sec}$



$T = 0.75 \text{ sec}$



$T = 1.00 \text{ sec}$



$T = \infty$

FIGURE 29 - EFFECT OF WAVE PERIOD ON SLICK SETUP. BOOM DEPTH = 4 in.
CURRENT = 1.2 fps; $V = 1.0 \text{ ft}^3/\text{ft}$; WAVE HEIGHT = 1.4 in.
DIESEL FUEL

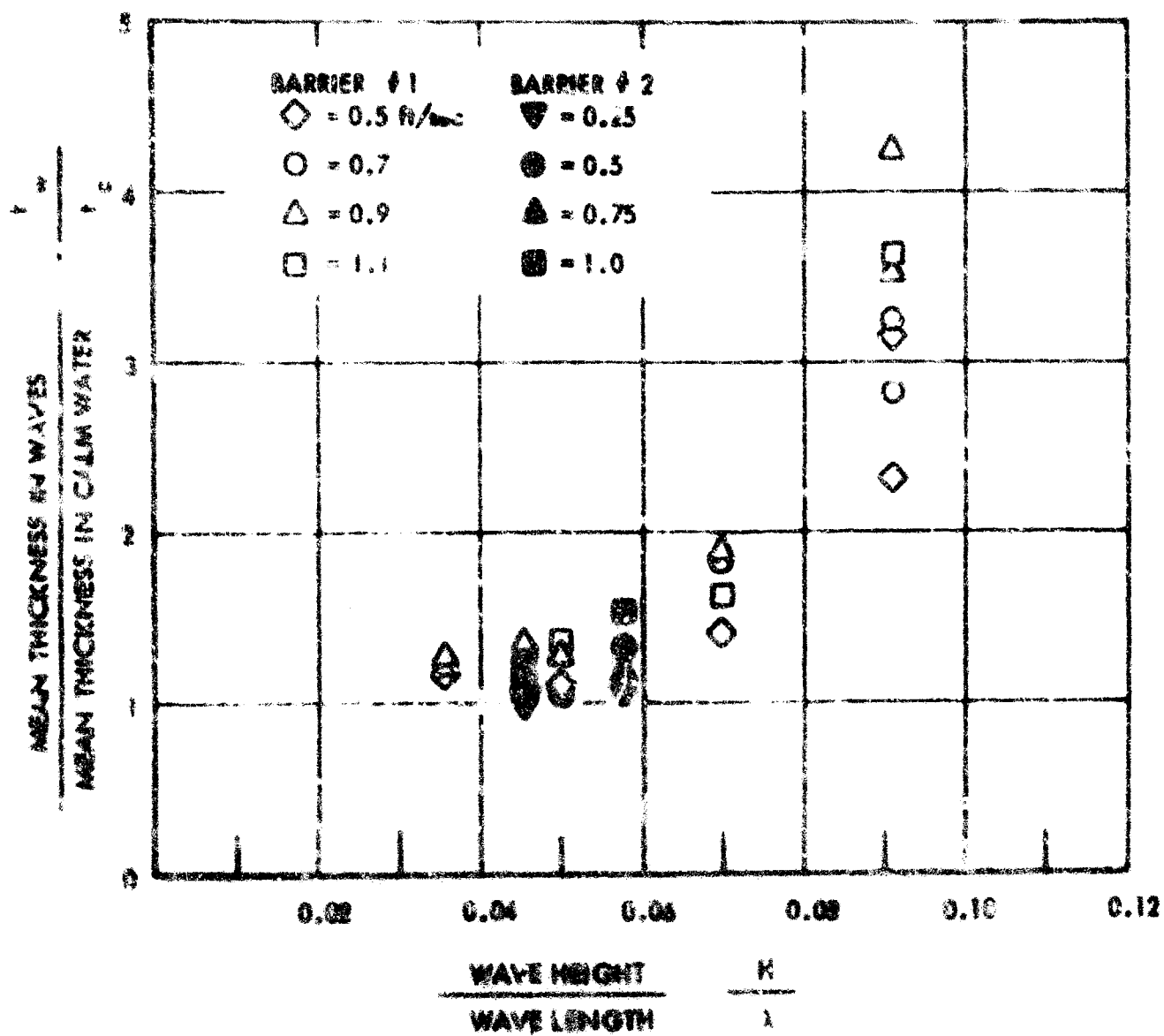


FIGURE 30 - EFFECT OF WAVES ON OIL SETUP

HYDRONAUTICS, INCORPORATED

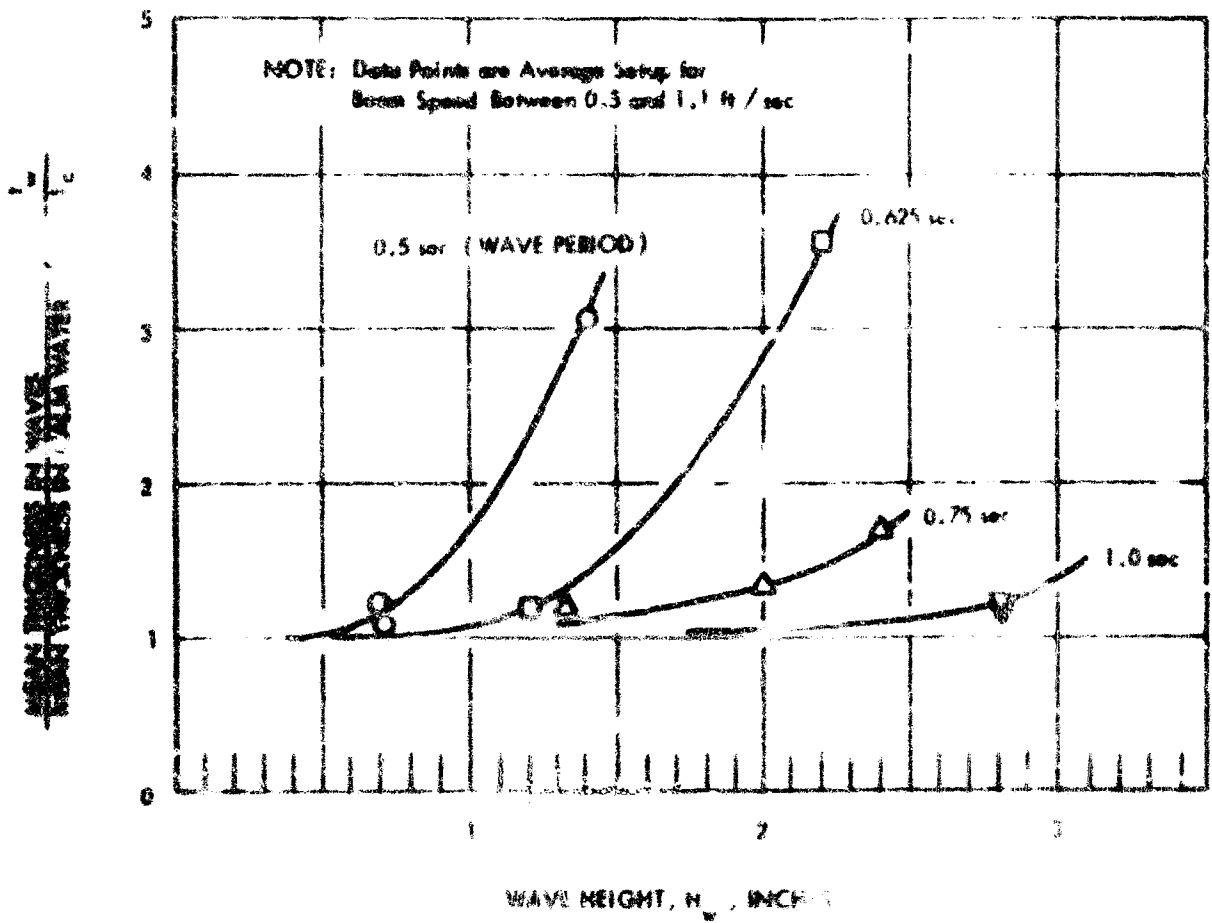


FIGURE 31 - OIL SETUP VS. WAVE HEIGHT AND PERIOD

HYDRONAUTICS, INCORPORATED



VELOCITY = 1.60 fps



VELOCITY = 1.40 fps



VELOCITY = 1.60 fps

FIGURE 32 - COMPARISON OF SLICK GEOMETRY IN SINGLE AND DOUBLE BOOM EXPERIMENTS. #2 DIESEL FUEL. VOLUME = 1.0 ft³/ft. BOOM SPACING = 9 ft. BOOM DEPTHS = 5 in. AFT BOOM AND 3.5 in. FWD BOOM.

HYDRONAUTICS, Incorporated

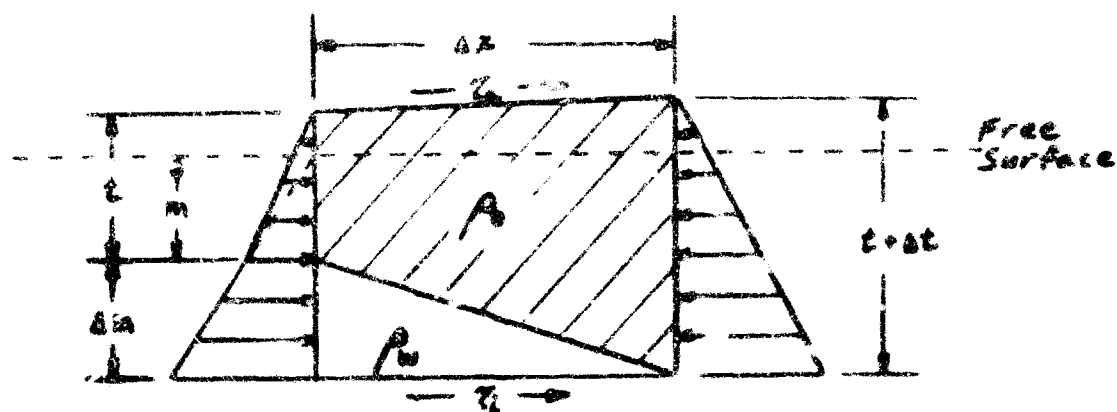
-67-

APPENDIX A
EQUATIONS FOR CONTAINED SLICK LENGTH

APPENDIX A

1. Differential Equation Governing Oil Slick Setup

The equation governing longitudinal thickening of the oil slick is derived by considering a differential control volume:



The horizontal forces on the control volume consist of the wind shear at the free surface τ_a , the interfacial shear τ_i , and the hydrostatic pressures at each end. The interface slope $\Delta m / \Delta x$ is assumed to be small so that the shears at the surface and interface are taken to act horizontally at the control surface boundaries. The slick thickness t is related to the depth of oil below the water free surface m :

$$m = \frac{\rho_o}{\rho_w} t$$

The equilibrium equation is given by.

$$\frac{1}{2} \rho_o g t^2 + \rho_w g \left(\tau + \frac{\Delta m}{2} \right) \Delta x + (\tau_1 + \tau_2) \Delta x = \frac{1}{2} \rho_o g (t + \Delta t)^2$$

Substituting for m and Δm , and rewriting

$$\begin{aligned} \frac{2(\tau_1 + \tau_2) \Delta x}{\rho_o g} &= (t + \Delta t)^2 - t^2 - \frac{\rho_o}{\rho_w} (2t \Delta t + \Delta t^2) \\ &= \left(1 - \frac{\rho_o}{\rho_w} \right) (2t \Delta t + \Delta t^2) \end{aligned}$$

Dropping the second order term Δ^2 and substituting g for

$$g \left(1 - \frac{\rho_o}{\rho_w} \right)$$

$$\frac{2(\tau_1 + \tau_2) \Delta x}{\rho_o g'} = 2t \Delta t$$

or

$$\frac{2\tau}{\rho_o g'} = 2t \frac{dt}{dx}$$

The interfacial slope is given by

$$\frac{ds}{dx} = \frac{\tau}{\rho_w g' t}$$

2. Simplified Model for Slick Length in Current Only

The maximum headwave thickness is specified by the headwave Froude number:

$$F_d = \frac{U}{\sqrt{g' t_h}} \Rightarrow t_h = \frac{U^2}{g' F_d^2}, \text{ ft}$$

The following relationships for headwave geometry are derived from Figure 21:

$$\text{headwave length, } l_h = 8 t_h, \text{ ft}$$

$$\text{headwave specific volume, } V_h = 5.64 t_h^3, \text{ ft}^3/\text{ft}$$

$$\text{slick thickness behind the headwave, } t_1 = 0.6 t_h, \text{ ft}$$

We now make the simplifying assumption that the interfacial shear stress is constant along the slick behind the headwave starting where $t = t_1$, i.e., $x = 0$. Then, using the differential equation derived above in integral form:

$$\int_{t_1}^{t(x)} 2t \, dt = \int_0^x \frac{2\tau}{\rho_0 g'} \, dx$$

$$\therefore t(x)^2 - t_1^2 = \frac{2\tau_1}{\rho_0 g'} x$$

NOTE: $\tau = \tau_1$ because τ_a is assumed = 0.

HYDROMAUTICS, Incorporated

-71-

$$\text{or} \quad t(x)^2 = \frac{2\tau_1 x}{\rho_0 g'} + t_1^2$$

$$= Kx + t_1^2$$

$$\text{where} \quad K = \frac{2\tau_1}{\rho_0 g'} = \frac{2}{\rho_0 g'} (C_f \cdot \frac{1}{2} \rho_w U^2) = \frac{C_f U^2}{g'}$$

C_f = effective interfacial friction coefficient, and

The specific volume behind the headwave is obtained by integrating thickness $t(x)$.

$$\Psi_x = \int_0^x t(x) dx = \int_0^x (Kx + t_1^2)^{\frac{1}{2}} dx$$

$$= \frac{2}{3K} \left[(t_1^2 + Kx)^{3/2} - t_1^3 \right]$$

The total slick length l_s and volume Ψ_s are found using:

$$l_s = l_h + x$$

$$\Psi_s = \Psi_h + \Psi_x$$

A listing of the computer program using this simplified model for slick length follows in Appendix B.

HYDRONAUTICS, Incorporated

-72-

APPENDIX B

COMPUTER PROGRAM FOR CALCULATING SLICK
CHARACTERISTICS AND ENTRAINMENT LOSS RATE

APPENDIX B

COMPUTER PROGRAM FOR CALCULATING SLICK
CHARACTERISTICS AND ENTRAINMENT LOSS RATE

A computer program has been written to calculate the characteristics of an oil slick and the entrainment loss rate as a function of current speed. The formulations used in these calculations are described in Section III and Appendix A of this report. The input to this computer program is as follows

Card 1 Format F10.2

| | | |
|-----|--|---------------------|
| FD | Froude number at which headwave propagates | N.D. |
| CF | Friction coefficient at the interface | N.D. |
| SG | Specific gravity of the oil | N.D. |
| VOL | Specific volume of oil contained | Ft ³ /ft |

Card 2 Format F10.2

| | | |
|------|---|----------------------|
| RHOW | Mass density of water | Slug/ft ³ |
| VISO | Viscosity of the oil | Ft ² /sec |
| SIG | Interfacial tension between oil and water | Lb/ft ² |
| CE | Headwave entrainment coefficient β' | N.D. |

Card 3 Format F10.2

| | | |
|----------------|---|--------|
| UC(1) to UC(6) | Current speed at which characteristics are required | Ft/sec |
|----------------|---|--------|

A sample output is given below. The slick length and thickness (at the boom end of the slick) are given in feet and the loss rate in cubic feet per second per foot of boom. In the event that the volume given is not sufficient to fill the headwave at a given speed, the message "slick unstable" is printed out. A listing of the computer program follows.

EXAMPLE OUTPUT

ESTIMATE OF SLICK CHARACTERISTICS AND ENTRAINMENT LOSS RATE

FD= 1.140 CF=0.004000 SG= 0.860 VOL= 0.800

RMOW= 1.940 VISU=0.0000400 SIG=0.00110000 CE= 0.0100000

| SPEED | SLICK L TH | THICKNESS | LOSS RATE |
|-------|------------|-----------|-----------|
| 2.00 | 14.66 | 0.47 | 0.000733 |
| 2.10 | 17.46 | 0.50 | 0.003551 |
| 2.20 | 16.40 | 0.53 | 0.008739 |
| 2.30 | 14.97 | 0.57 | 0.018295 |
| 2.40 | 13.65 | 0.60 | 0.033209 |
| 2.50 | 12.43 | 0.64 | 0.076232 |

PROGRAM LISTING

```

77 FIM
*IOCSICAND,1403 PRINTER)
*LIST ALL
C PROGRAM TO ESTIMATE OIL SLICK CHARACTERISTICS AND ENTRAINMENT
C LOSS RATE AS A FUNCTION OF CURRENT SPEED
REAL R
DIMENSION UC(16)
100 READ(7,1)FD,CF,SG,VOL
READ(7,1)RMOW,VISU,SG,CE
READ(7,1)UC(1),UC(2),UC(3),UC(4),UC(5),UC(6)
1 FORMAT(10,2)
WRITE(5,110)
110 FORMAT(1H, ' ESTIMATE OF SLICK CHARACTERISTICS AND ENTRAINMENT LO
1SS RATE ')
WRITE(5,111)FD,CF,SG,VOL
111 FORMAT(1H, ' FD=,F6.3, ' CF=,F6.6, ' SG=,F6.3, ' VOL=,F10.3)
WRITE(5,112)RMOW,VISU,SG,CE
112 FORMAT(1H, ' RMOW=,F8.3, ' VISU=,F10.8, ' SG=,F10.8, ' CE=,F10.7)
WRITE(5,113)
113 FORMAT(1H, ' SPEED, F10, ' SLICK L TH, F25, ' THICKNESS, F40, ' LOSS RATE
114
DO 10 J=1,6
GP=12,17+1,-56)
TH=UC(J)/FD**2/GP
XLM=0.0TH
VH=4.62*TH**2
T1=0.6*TH
N=11*UC(J)**2/SG/GP
VX=VH-VH
IF(VX)20,20,11
VX=VX*K*1.5*T1**3
VX=VX**0.6667-11**2
X=VX/K
XLS=XLM*X
TH=(T1**2*K*X)**0.5
DMIN=7.26*SIG/UC(J)**2*(1.0/(RMOW*SG*VISU*UC(J)/SG)**.7)
DMAX=4.0DMIN
VRC=.75*TH*UC(J)/X
D1=1VRC/1.741**2/GP
D2=1VRC*.0000112**4/(1.153*GP**7111**0.875
D3=1VRC*18.0*0000112/GP)**.5
IF(D1-D2)12,12,13
12 IF(D2-D3)14,14,15
13 DCRIT=D1
GO TO 14
14 DCRIT=D3
GO TO 14
15 DCRIT=D2
VL=CE*UC(J)*TH
UC=4.2*(SIG*GP/RMOW)**.25
IF(UC(J)-UD)30,30,40
30 VE=0.0
GO TO 50

```

PAGE 2

```

40 IF(DMIN-DCRIT)41,41,42
42 VE=0.0
GO TO 50
41 IF(DMAX-DCRIT)43,43,44
44 VE=VL*(DCRIT-DMIN)/(DMAX-DMIN)
GO TO 50
53 VE=VL
50 WRITE(5,114)UC(J),XLS,TH,VE
114 FORMAT(1H, 'F5.2,F10,F10.2,F25,F10.2,F40,F10.6)
GO TO 10
20 WRITE(5,115)UC(J)
115 FORMAT(1H, 'F5.2, ' SLICK UNSTABLE ')
10 CONTINUE
GO TO 100
END
VARIABLE ALLOCATIONS

```

HYDRONAUTICS, Incorporated

-75-

APPENDIX C
EXAMPLE OF LOSS CALCULATIONS

APPENDIX C

Example of Loss Calculations

Given: 3,000 ft boom
20,000 ton spill
Withdrawal system capable of collecting spill in 48 hours

Find: Current velocity in which system can operate with acceptable losses.

Analysis:

(1) Assume Properties of Oil

Specific Gravity, S.G. = 0.90

Kinematic Viscosity, $\nu = 10^{-3}$ ft²/sec

Interfacial Tension, $\sigma = 0.0011$ lb/ft²

Interfacial Friction Coefficient, $C_f = 0.010$

Headwave Froude Number, $F_d = 1.00$

Volume Loss Rate Coefficient, $\beta^1 = 0.0073$

Parabolic Boom Geometry as shown in Figure C-1

(2) Losses will be confined to relatively small lengths of boom at the corners where the boom intersects the headwave. Thus, assume that the angle, θ , between the boom axis and the current direction is constant in the loss regions.

(3) The specific loss rate as a function of slick length between the headwave and boom, and current velocity is computed using the program in Appendix B. Assume that the loss rate for slick lengths less than the headwave length is constant and

equal to the rate of droplet (volume) formation. The area under a curve of specific volume loss vs. slick length is proportioned to the loss rate divided by the slope of the boom ($\tan \theta$) at the corner. This loss rate (for both corners) is shown in Figure C-2 as a function of current speed. The maximum slick length for any significant entrainment loss is also shown.

(4) The simplified theory for setup given in Appendix A is used to generate the curves of specific volume vs. slick length shown in Figure C-3. These curves are used to calculate, by numerical integration, the contained volume shown in the figure for the assumed boom geometry. The contained volume is shown as a function of slick length which should be taken as the maximum length, i.e., at the apex.

(5) The volume of the oil spill and the withdrawal rate are:

$$\text{Volume} = \frac{20,000 \times 2,200}{62.4 \times .90} = 7.85 \times 10^5 \text{ ft}^3$$

$$\text{Pump Rate} = \frac{7.85 \times 10^5}{48 \times 3,600} = 4.55 \text{ ft}^3/\text{sec}$$

(6) The curves of contained volume are entered to determine the slick length at the apex. The slope of the boom at the headwave leading edge is calculated. The loss rate from Figure C-2 is multiplied by $\tan \theta$ to obtain the loss rate.

(7) The results are summarized in Table C-1 for the boom geometry shown in Figure C-1 and one additional configuration for which the parabola opening width has been reduced to 1330 ft.

Conclusions:

In order to obtain 99% recovery of oil collected in the boom, current must be less than 1.3 fps with the boom geometry shown in Figure C-1. At 1.5 fps the recovery would be less than 95%. By reducing the opening to 3400 feet, nominal current is increased to 1.5 and 2.0 fps for 99 and 95%, respectively.

The loss rate will increase as slick volume is decreased so that the slope at the intersection of the headwave and the boom increases. For example, at 1.4 fps, the loss rate (2260-ft. opening) after 24 hours is 0.074 ft³/sec compared with 0.063 ft³/sec at the beginning of operation. The increase is gradual and should be countered by decreasing the width of the boom opening as oil is recovered.

TABLE C-1
Results of Sample Calculations

| Room Opening, Ft | Current U, fps | Max. Slick Length, Ft | Width @ Leading Edge, Ft | tan θ @ 1.e | Loss Rate | |
|------------------------|----------------------|-----------------------------|--------------------------------|--------------------------|----------------------|-------------------|
| | | | | | Ft ³ /sec | % of Pump Rate |
| 2260 | 1.2 | 580 | 1860 | .81 | .004 | 0.09 |
| | 1.4 | 540 | 1800 | .84 | .063 | 1.39 |
| | 1.6 | 520 | 1750 | .86 | .146 | 3.22 |
| | 1.8 | 470 | 1680 | .90 | .290 | 6.59 |
| 1330 | 1.2 | 830 | 1110 | .34 | .0017 | 0.04 |
| | 1.4 | 770 | 1070 | .35 | .026 | 0.57 |
| | 1.6 | 720 | 1040 | .36 | .061 | 1.34 |
| | 1.8 | 670 | 1000 | .38 | .122 | 2.68 |

HYDRONAUTICS, INCORPORATED

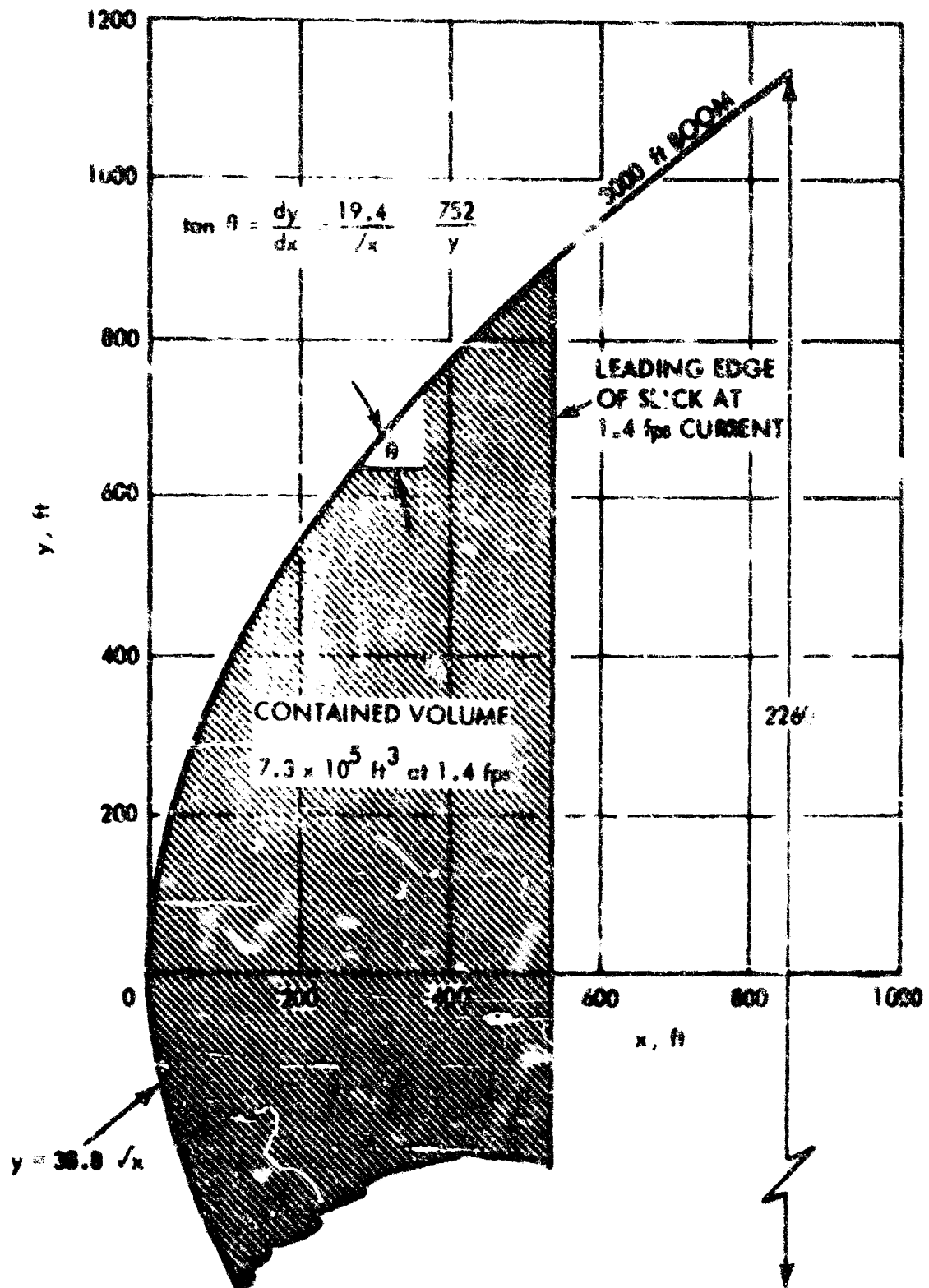


FIGURE C-1 ASSUMED BOOM GEOMETRY

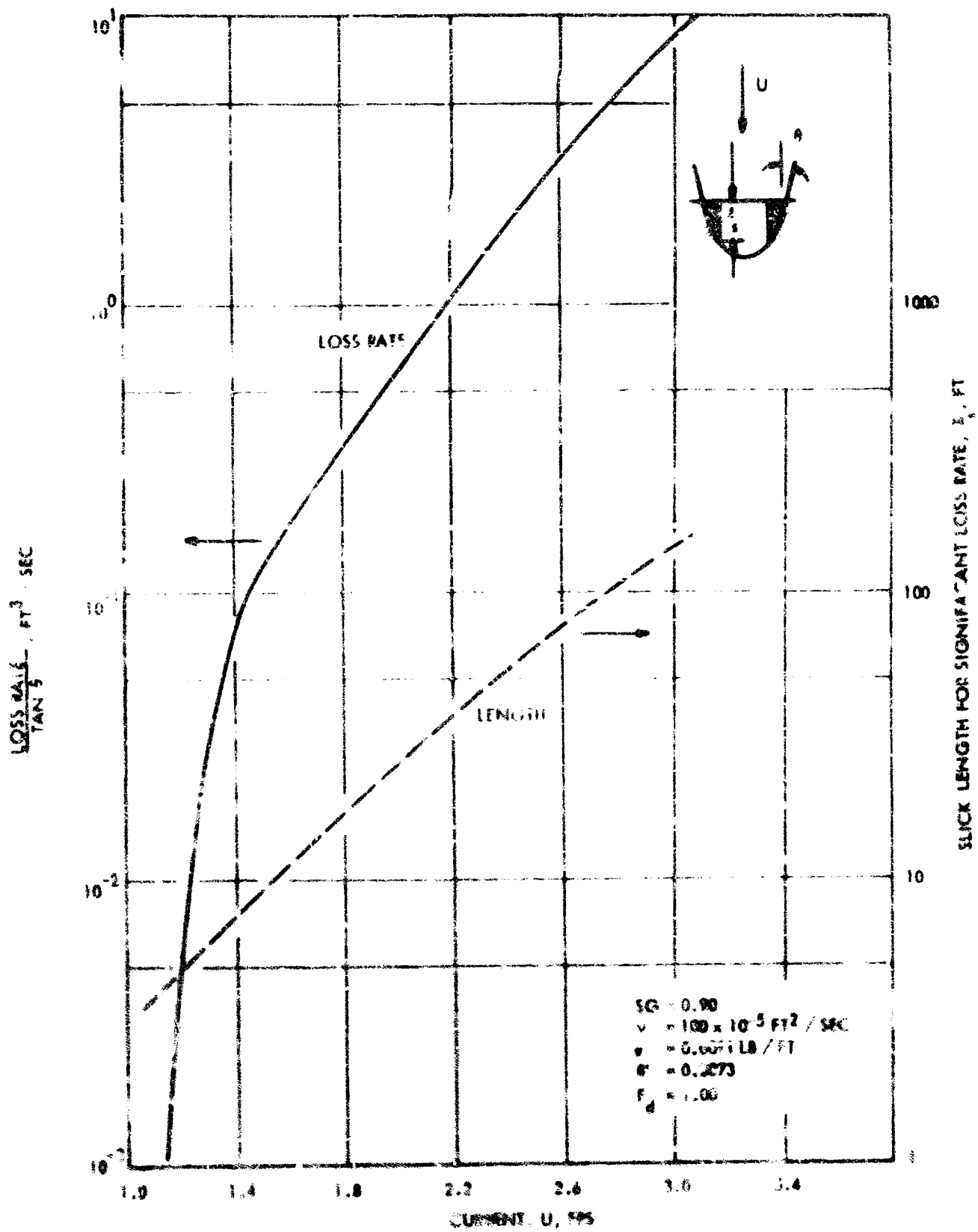


FIGURE C - 2 - ENTRAINMENT LOSS RATE IN COAMERS

HYDRONAUTICS, INCORPORATED

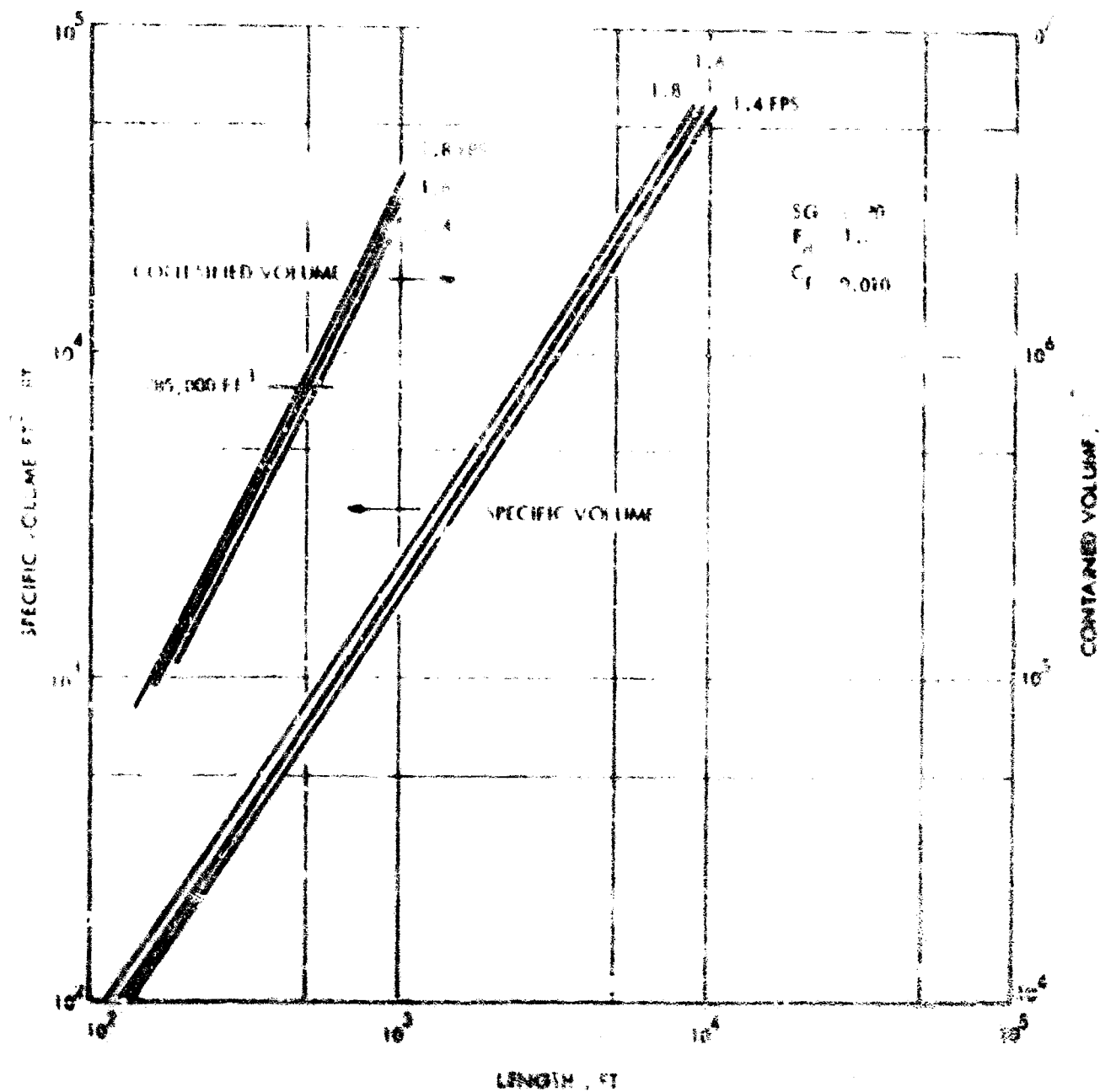


FIGURE C 3 SPECIFIC VOLUME AND CONTAINED VOLUME